SCREENING FOR EARLY KERATOCONUS IN PEDIATRIC PATIENTS WITH ASTIGMATISM

A thesis presented to the graduate faculty of
New England College of Optometry in partial fulfillment
of the requirements for the degree of Master of Science

Hannah E. Milikich

May 2026

SCREENING FOR EARLY KERATOCONUS IN PEDIATRIC PATIENTS WITH ASTIGMATISM

Hannah E. Milikich

This manuscript has been read and accepted by the
Thesis Committee in satisfaction of the
thesis requirement for the degree of Master of Science

5/12/2026
Date

Signed by:
Hillary L.G. Baker
939723ECF56944A...
Hilary L.G. Baker, OD, MSc
Graduate Faculty Advisor

DocuSigned by:
Kristen L. Kerber
459AE881FB8A4ED...
Kristen Kerber, OD, MS, FAAO
Thesis Committee Member

DocuSigned by:
Sangeetha Metlapally
EF5BE7B05D3D4CA...
Sangeetha Metlapally, PhD, BSOpt, FAAO
Thesis Committee Member

DocuSigned by:
Angelica Scanzera
A9909E2EFA58451...
Angelica C. Scanzera, OD, MPH, FAAO, FSLS
Thesis Committee Member

5/12/2026
Date

DocuSigned by:
78A8AD972399447...
Athanasios Panorgias, MS, PhD
Director of Graduate Studies

Abstract

SCREENING FOR EARLY KERATOCONUS IN PEDIATRIC PATIENTS WITH ASTIGMATISM

Hannah E. Milikich

New England College of Optometry, 2026

Introduction:

Pediatric keratoconus (KC) is often more aggressive than adult KC, and recent studies suggest its prevalence is higher than previously thought. Topography is commonly used to screen for KC, however tomography is the gold standard for diagnosis of manifest and subclinical KC. Currently, tomography is not readily accessible to all clinicians. The purpose of this study is to investigate corneal characteristics of astigmatic children flagged as keratoconus suspects based on topography to better understand which indices may better predict early KC detection.

Methods:

Patients (n = 164 eyes) aged 5-18 (mean 10.83 ± 3.89) years with at least 1D of cylinder (2.28 ± 0.94D) were recruited from a community health center. Corneal topography, aberrations, and pachymetry at central, steepest, and inferior locations were measured with the Topcon Corneal Analyzer CA-800 and the Zeiss Cirrus HD-OCT 500. T-tests were performed to analyze differences between low and high cyl groups, and KC suspects and

non-suspects; and linear models were used to determine which corneal indices were better predictors of keratoconus probability index (KPI). KC suspects were defined by a minimum KPI of 23%.

Results:

Subjects were divided into either high cyl (≥2.5D) or low cyl (<2.5D) groups, and significant differences were found between high cyl (mean -4.42 ± 0.89D) and low cyl (-2.12 ± 0.66D) groups for K cyl, steep K, SAI (surface asymmetry index), total aberrations, and higher order aberrations. Subjects flagged as KC suspects had higher K cyl, SAI, total aberrations, and increased age. Linear models were compared and according to p-values and adjusted r-squared values the best overall model other than one containing all data points used the 3 metrics age, AGC (apical gradient curvature), and SD (standard deviation of corneal power) ($r^2 = 0.374$).

Discussion:

No significant difference was found between refractive cyl groups and incidence of suspected KC, and KC suspects had steeper corneas, more irregular corneal surfaces, older age, more negative spherical equivalent refractive error, and more corneal aberrations. KPI was best predicted by a combination of all data points, and a model using age and corneal indices AGC and SD performed similarly. This study suggests that these features may be good predictors of early KC and incorporated into a disease severity classification system, though further research is needed to describe KC classification and best practices for screening for suspects.

Acknowledgements

First and foremost I would like to thank my mentor, Dr. Hilary Baker, who has been absolutely essential in the process of my completion of this project as a personal and professional mentor and friend, and whose help I am particularly grateful for.

I would also like to thank Dr. Stacy Lyons, who assisted in the creation of the posters presented at Academy and ARVO 2025, and was the attending optometrist for all the pediatric patients who were enrolled as subjects in this study. She oversaw their management and has impacted countless young lives.

I would also like to thank the members of my thesis committee, Dr. Kristen Kerber, Dr. Sangeetha Metlapally, and Dr. Angel Scanzera, for their input and expertise in the finalization and communication of the findings of this project.

Thank you to Dr. Chris Taylor, who was an enormous help in the data analysis for this project and translating the raw data into meaningful information.

While I had much professional help in the course of completing this thesis, the impact of personal support cannot be overstated and I would like to thank my friends and classmates from NECO in the OD and MS programs who kept me sane and grounded me during the difficult process of obtaining two graduate degrees simultaneously, and I am eternally grateful to have your companionship.

Last but certainly not least, thank you to my family, particularly my parents, who have supported me my whole life in every possible way, and given me more than anyone should ever be asked to give.

Table of Contents

List of Figures and Tables

1. General Introduction

Keratoconus (KC) is a corneal disorder characterized by ectasia, progressive thinning, dysregulation at all cellular layers, irregular astigmatism, and reduced vision (Gomes et al. 2015). It typically appears in young adulthood or childhood around puberty, but pediatric KC is typically more aggressive and progresses faster than that of adult patients (Mukhtar and Ambati 2017). Detection currently relies on topographical measurement and tomography is the gold standard in diagnosis (Gomes et al. 2015), and it can be difficult to detect, especially in early stages (Anitha et al. 2021; Gomes et al. 2015). A published case report describes several pediatric patients with KC who were previously diagnosed with meridional amblyopia due to the presence of high amounts of refractive cyl, inability to fully correct vision with glasses, and lack of detection of corneal characteristics (Arora and Lohchab 2019). Misdiagnosis of KC can lead to lack of proper intervention and thus disease progression (Léoni-Mesplié et al. 2012). It is important to have guidelines in place regarding signs that would indicate presence of early, subclinical, or preclinical KC (Shi 2016), but this disease has historically been under-investigated and there is a lack of concrete guidelines in place for practitioners regarding definitions of disease staging, classification, and best practices for detection and management (Gomes et al. 2015).

1.1 Keratoconus

1.1.1 Epidemiology

The prevalence of KC is now thought to be much higher than previously reported due to more advanced detection techniques - historically a frequently cited prevalence is 1 in 2,000

(Kennedy et al. 1986; Kymes et al. 2004; Mukhtar and Ambati 2018; Romero-Jiménez et al. 2010), which is based on a registration study conducted in the US from 1935 until 1982. The first population-based report of KC prevalence via screening from 1959 reported a prevalence of 0.6% (Hofstetter 1959). However, more recent studies report a range of prevalence varying by geographic location and ethnic group, up to 40 in 1,000 (Harthan et al. 2024; Hashemi et al. 2020). An epidemiologic study from 2016 conducted in the Netherlands reported age-specific incidence of 1 in 7,500 and prevalence of 1 in 375 (Godefrooij et al. 2016). The prevalence tends to be much higher in South & Southeast Asian and Middle Eastern populations, and there is no clear difference in sex distribution (Anitha et al. 2021).

Important risk factors for KC include Down's syndrome, family history, ocular allergy, ethnicity (specifically Asian and Arabian), mechanical factors (eye rubbing), floppy eyelid syndrome, atopy, and connective tissue disorders such as Marfan syndrome and Ehlers-Danlos (Gomes et al. 2015). KC has a number of ocular and systemic associations. Ocular associations include blue sclera, ectopia lentis, cataracts, retinal detachment, retinitis pigmentosa, macular coloboma, Leber's congenital amaurosis, aniridia, vernal keratoconjunctivitis, and atopic keratoconjunctivitis. Systemic associations include Down's syndrome and Ehlers Danlos (Anitha et al. 2021). There is no agreed-upon direct relationship between KC and dry eye (Gomes et al. 2015). KC typically develops in the second decade of life in which the cornea becomes unstable and develops an irregular, often conical shape, and changes in myopia, irregular astigmatism, and higher-order aberrations manifest. It typically progresses until the third or fourth decade of life when the disease process generally

stabilizes (Buzzonetti et al. 2020). There is a possibility for spontaneous stabilization of KC with age, but this is rare (El Rami et al. 2015; Mukhtar and Ambati 2018).

Most literature agrees that younger patients have a higher incidence of rapid progression than adults - a study by Chatzis and Hafezi in 2012 reported 88% of pediatric KC patients progressing; however, some literature disputes that a younger age is correlated with faster progression (Dana et al. 1992; Woodward et al. 1990). In pediatric patients, early diagnosis is needed to prevent many complications of the disease including ectasia progression requiring corneal transplantation, central opacities and scarring, and severe visual loss (Ertan and Muftuoglu 2008). Based on this information, it is important to know which parameters best detect disease progression in children. The indicators used with children generally include changes in max keratometry (Kmax), refractive astigmatism (cyl), and corrected distance VA (CDVA) (Chatzis and Hafezi 2012; Hashemi et al. 2022; Sylvain et al. 2016).

1.1.2 Pathogenesis and Histopathology

Overall, the pathogenesis of KC is poorly understood, although it is often described as a multifactorial condition involving genetic, metabolic, and environmental factors. The longstanding and currently accepted definition is that it is non-inflammatory (Krachmer et al. 1984), however recent research has displayed the role of various inflammatory mechanisms. Generally agreed-on main causative factors include genetics, environmental factors, inflammation, enzymes, oxidative stress, and hormones (Anitha et al. 2021).

KC has a high association with allergies, and vernal keratoconjunctivitis (VKC) is the most commonly associated ocular allergy. Although the mechanism of KC development is largely

unknown, allergen exposure, eye rubbing, and epithelium microtrauma can cause KC development and increase the release of inflammatory mediators, such as MMP-1, from the epithelium and stroma (Anitha et al. 2021; Buzzonetti et al. 2020). The association of KC with connective tissue disorders is related to the potentially inflammatory nature of the disease: a cross-linking enzyme lysyl oxidase (LOX) is commonly reduced in KC patients, and in patients with these connective tissue disorders, KC may arise because of a generalized and complex disorder of connective tissue (Dudakova and Jirsova 2013).

Hormones are also thought to be involved in KC development, specifically the sex hormones estrogen and progesterone, and thyroid hormone T4, or thyroxine (Ayan et al. 2019; Thanos et al. 2016). Generally, the onset of KC approximately aligns with puberty, following major changes in hormones. Additional factors suggesting that hormones play a role in KC include the fact that corneal ectasia progresses during pregnancy, and corneal thickness and hysteresis vary during the menstrual cycle (Anitha et al. 2021; Ayan et al. 2019).

Abnormalities can be documented in almost every layer of a cornea affected by KC: the epithelium thins and displays irregular loss of basal cells, with apoptotic cells present over the cone; Bowman's layer shows breaks and fibrillations; the stroma displays altered orientation of collagen fibrils, loss of lamellae, increased visibility of nerve fibers due to corneal thinning, and thickening of nerve fibers; and Descemet's ruptures and folds (Santodomingo-Rubido et al. 2022). There is controversy regarding whether the endothelium is affected in KC (Santodomingo-Rubido et al. 2022) because cell density is often unaffected (Efron and Hollingsworth 2008; El-Agha et al. 2014; Weed et al. 2007), but it may display

abnormal signs including intracellular dark structures, pleomorphism, and cell elongation (Anitha et al. 2021); additionally, a decrease in endothelial cell density in severe KC (Mocan et al. 2008; Uçakhan et al. 2006) has been reported. More advanced disease stages of KC produce corneal signs including Vogt's striae, Fleischer ring, scarring, and central dense corneal stromal edema (hydrops) due to tears in Descemet's (Buzzonetti et al. 2020; Krachmer et al. 1984).

1.1.3 Detection

Suspicion for KC is typically based on topographical measurement and tomography is the gold standard in diagnosis (Gomes et al. 2015).

1.1.3.1 Topography

Topography involves taking an image of the front of the eye, producing what is essentially an elevation map detailing the contour of the eye (Cavas-Martinez et al. 2016). Topography also produces indices based on specific measurements of the cornea. These indices vary across devices, and typically describe corneal steepness and asymmetry. Poor repeatability of these topographic indices is often a sign of dry eyes and increased optical aberrations, which can be associated with corneal ectasia and may warrant further investigation for presence of KC (Masiwa and Moodley 2020; Shankar et al. 2008).

There are three main technologies employed by current topographers: those based on light reflection on the cornea, those based on the projection of a slit of light on the cornea, and those based on the reflection of multicolor LEDs on the cornea (Cavas-Martinez et al. 2016).

Usually, topographers employ Placido discs, rings of light with standard size and spacing, which are reflected on the anterior surface of the cornea and the image captured by a camera and analyzed digitally, with variations from the standard size comprising the variations in shape and curvature measured. This process is used to compare the measured three-dimensional shape of the cornea to a reference shape, and differences are displayed using a color scale developed in a study (Maldonado et al. 2006); the topographer used in this study uses Placido-based technology to capture corneal shape and then applies further calculations to determine various corneal indices.

1.1.3.1.1 Univariate Topographic Indices

Corneal topography is very useful in detecting and describing corneal disease because it is able to create a detailed three-dimensional map of the shape of the cornea, as well as quantitatively describe certain morphological features through the use of numerical indices (Cavas-Martinez et al. 2016). Univariate indices involve either a simple description of some feature of the cornea, or are derived from a single-step calculation.

Corneal astigmatism (K cyl) was one of the indices measured by the topographer during scans. Simulated keratometry (SIMK) contains information on values of the dioptric curvature of the flat and steep meridians, K1 and K2, within the clinically useful region of the cornea, diameters of Placido rings between 3 and 9mm eccentricity. K cyl is calculated simply by taking the difference between the dioptric curvature values of the flat and steep meridians, K1 and K2 (Cavas-Martinez et al. 2016). Steep K is a value based on SIMK, which is calculated from information about the elevation across the corneal surface

reconstructed algorithmically to determine height and slope, from which curvature meridians are identified and labeled as K1 and K2, corresponding to flat and steep.

Apical, or apex, curvature (AK) represents the corneal power at its apex (Cavas-Martinex et al. 2016). A value less than 48 D is considered normal, between 48 and 50 D suspect, and greater than 50 D significantly high (Cavas-Martinex et al. 2016). Kc is the central corneal curvature, based on the selected pupil size (Topcon 2024). Both AK and Kc are essentially ways of describing the maximum corneal steepness.

Apical gradient curvature, or AGC, is a topography index that describes how quickly the corneal power changes in relation to the central, or apical, corneal power. Higher values (greater than 2 D/mm) are highly correlated with KC, with values less than 1.5 being normal (Cavas-Martinez et al. 2016). Since AGC essentially describes how quickly the corneal power or steepness changes as one gets further from the center of the cornea, and higher values tend to predict KC, it was expected that this would be a good predictor of KC.

According to Topcon, whose technology was used in this study, the index SD represents the cornea's curvature irregularity expressed as the standard deviation of curvature over a central 4.5mm area (Topcon 2024). SD is an additional way to describe the irregularity of curvature of the anterior cornea, which is associated with development and progression of KC (Buzzonetti et al. 2020), so this finding is unsurprising and agrees with current literature.

Superior-inferior (SI) compares the average curvature of 2 matched zones in the superior and inferior cornea to display differences between the two (Topcon 2024). A similar index is the I-S index, described by Rabinowitz as being an average of three data points on three

topographic rings 3 mm superior and inferior to the central cornea 30º apart, with the superior value subtracted from inferior. A positive value for SI or I-S indicates the cornea is steeper inferiorly, and a negative value indicates the cornea is steeper superiorly (Rabinowitz 1995).

Surface asymmetry index (SAI) is a univariate index that is calculated as the average of the curvature power difference between points 180º apart on 128 evenly spaced meridians on the corneal surface. A perfect spherical shape would have a value of zero, with power on each meridian being equal; a higher value indicates higher asymmetry (Cavas-Martinez et al. 2016). SAI describes the overall asymmetry of the curvature of the cornea rather than asymmetry when comparing specific areas, as is the case with the SI index which specifically describes inferior-superior asymmetry. Higher corneal surface asymmetry is associated with KC (Hashemi et al. 2022), so as it was hypothesized that suspected KC incidence would be correlated with higher cyl, higher SAI would also be correlated with higher cyl.

1.1.3.1.2 Multivariate Topographic Indices

Multivariate indices are calculated from statistical analysis of several other indices using linear discriminant function to differentiate between two conditions, such as KC and non-KC (Maeda et al. 1994). Several multivariate indices have been created to diagnose KC based on differing compositions of univariate indices.

KPI is a topographical index that is based on multivariate statistical analysis taking into account all other corneal characteristics and giving a final value for how likely it is that the measured eye has KC (Maeda et al. 1994). According to Topcon, KPI is calculated based on

the indices AK, AGC, and SI (Topcon 2024). Studies have established an accepted threshold value for this index of 23%, meaning that any eye with a KPI of at least 23% may be flagged as a KC suspect (Maeda et al. 1994; Shi 2016). However, further research is needed to determine which KPI level is most effective to determine KC suspicion, as no consensus currently exists. One study defined subclinical KC by the presence of major and minor criteria, with a KPI of 23-30% qualifying as a minor criterion, and KPI >30% a major criterion (Jafarinasab et al. 2015).

Maeda et al. also created a version of KPI, or KC Prediction index. The calculation of KPI is described by Maeda et al. in a 1994 paper as "a linear discriminate analysis of eight quantitative topographic indices," including DSI, OSI, and CSI, which are calculated by dividing a map of the cornea into eight pie-shaped sectors, each subtending 45º. These terms are described in detail in Table 5. (Maeda et al. 1994).

Table 5: Description of Topographic Indices Included in Calculation of KPI per Maeda et al.

Index	**Term**	**Definition**
DSI	Differential sector index	The greatest difference in average power between any two sectors
OSI	Opposite sector index	The greatest differences in average power between any two sectors that are 180º apart
CSI	Center/surround index	The difference in the average corneal power

		between the central area and an area surrounding it
IAI	Irregular astigmatism index	The "average summation of inter-ring area-corrected power power variations along every semimeridian for the entire analyzed surface"
AA	Analyzed area	The "ratio of the interpolated data area to the area circumscribed by the last mire… in a videokeratoscopic image"
SimK1	Simulated K1	Dioptric curvature of the steep meridian
SimK2	Simulated K2	Dioptric curvature of the flat meridian
SAI	Surface asymmetry index	The average of the curvature power difference between points 180º apart on 128 evenly spaced meridians on the corneal surface

Other multivariate indices include the Belin/Ambrosio Enhanced Ectasia Display III (BAD III), which is used on many tomography scan results and is composed of nine indices displayed individually as well as combined in discriminant analysis and regression to differentiate KC from healthy corneas (Cavas-Martinez et al. 2016).

The keratoconus index, KCI%, also called the Klyce-Maeda method, creates a classification tree based on eight videokeratoscopic indices (Maeda et al. 1994). The Chastang method combines SDSD (the standard deviation of standard deviations of radii of curvature of each of 8 topographic corneal rings) and Asph (coefficient of asphericity within a 4.5mm pupil) indices to produce a primary decision tree (Cavas-Martinez et al. 2016; Chastang et al. 2000).

Keratoconus severity index, KSI, also called the Smolek-Klyce method, uses an algorithm based on a neural network derived from 10 topographic indices. The resultant numerical output classifies corneas as healthy, suspect KC, or manifest KC (Cavas-Martinez et al. 2016; Smolek and Klyce 1997).

The KISA % index is derived from 4 indices: the K value, IS, AST (which is SimK1 - SimK2 and describes regular corneal astigmatism), and SRAX (which is the skewed radial axis index and expresses irregular astigmatism) (Rabinowitz and Rasheed 1999). The goal in creating this index was to have an algorithm to detect and predict KC based on as little topographic criteria as possible, and is accepted as a useful screening tool for raising suspicion for KC using only topography (Cavas-Martinez et al. 2016).

The Rabinowitz and McDonell Index was one of the first multivariate KC detection systems created, and is based on I-S, central K, and the difference between central K of both of the patient's eyes (Cavas-Martinez et al. 2016; Rabinowitz 1995).

1.1.3.1.1 Other Indices and Data Points

When capturing topographic scans of subjects' eyes, the topographer also measures and quantifies aberrations. In order to measure aberrations, the topographer uses the recreated shape of the subject's cornea to simulate deviations that would occur from a perfectly symmetrical spherical wavefront path when a perfect reference wavefront passes through each point on the cornea. The path length difference between the reference wavefront and the subject's wavefront comprises the subject's corneal aberrations (Carvalho 2005).

These corneal aberrations can be used to characterize corneal regularity. The impacts of the cornea's shape on the wavefront aberration are described by decomposing the wavefront into several polynomials of various radial orders. The model used in this study employs Zernike analysis and provides 36 polynomials up to 7th order arranged as a pyramid, allowing for a more complete description of the optics of the eye via their orthogonality (Carvalho 2005).

Some of these individual polynomials describe aberrations well-known in the clinic for their negative impacts in KC, including defocus (myopia), astigmatism, spherical aberration, and coma. Defocus is a rotationally symmetric description of image rays coming to focus at different longitudinal points along a visual axis (Mahajan 1991). Primary astigmatism describes the difference in defocus between meridians caused by asymmetry of the refracting surface, in this case the cornea, with regular axes 90º apart. Spherical aberration results from failure of paraxial and peripheral rays to focus at the same point. Coma is a result of differing focal lengths of off-axis paraxial and peripheral rays (Asimellis 2019, 2022).

Aberrations are sometimes combined into a single number or statistic to describe the magnitude of aberrations, such as higher order root mean square (HORMS) aberrations (a combination of aberrations third order and above), or simply total root mean square (RMS) aberrations. KC causes increases in myopia, irregular astigmatism, and higher order aberrations, particularly spherical aberration, and coma (Omar 2019).

When research is conducted in the field of optics, refractive error must be considered in a way that allows for valid analysis. The terms used most commonly clinically of sphere, cylinder, and axis, cannot be statistically compared and analyzed because they are not independent, or orthogonal. In order to allow for separate analysis of the components of refraction, each component was transformed from sphere, cylinder, and axis into the vector components M, J0, and J45, which are orthogonal and may be analyzed individually (Pesudovs et al. 2007). The M vector is spherical equivalent, and J0 and J45 are Jackson crossed cylinder components with power at 180 and 45 degrees respectively - essentially, J0 represents the with (WTR) and/or against the rule (ATR) components, and J45 represents the oblique component (Liu et al. 2011).

1.1.3.2 Tomography, Pachymetry, and OCT

Tomography is an imaging method that can examine corneal curvature and thickness, and produces a more detailed scan of the three-dimensional shape of the cornea (Gomes et al. 2015). Tomography commonly employs Scheimpflug imaging, which enhances depth of focus without distorting the image, as well as automatically aligning captured images and compensating for eye movements (Ambrosio 2011).

Optical coherence tomography, or OCT, is a high axial resolution cross-sectional imaging technology that uses near-infrared spectral light and measures backscattered light to produce cross-sectional images of the tissue of interest (Aumann et al. 2019). Fourier domain OCT (FD-OCT) employs Fourier transformation to convert the signal into spectral information, capturing depth information in a single scan, providing much improved efficiency (Aumann et al. 2019; Shan et al. 2019). This technology evolved into two more efficient forms commonly in use today, spectral domain OCT (SD-OCT) and swept source OCT (SS-OCT). SD-OCT captures spectral information during scans, and uses a spectrometer to separate wavelength information from a scan (Aumann et al. 2019). SS-OCT was developed shortly after SD-OCT and sweeps the wavelength of the light source, which is then captured by a point detector, providing scanning capabilities without the need for moving parts, allowing for much higher rates of speed of image acquisition (Shan et al. 2019), and much higher signal-to-noise ratio, improving image quality vastly (Aumann et al. 2019).

Anterior segment OCT (AS-OCT) was developed and adapted from posterior imaging with slightly different imaging requirements, such as the need for larger width and depth scans than needed in posterior imaging (Shan et al. 2019). AS-OCT employs FD-OCT imaging of the anterior segment, though these devices require a lens adapter (Shan et al. 2019). SS-OCT for anterior segment imaging is also available, with much higher scan rates and width (Shan et al. 2019).

Corneal pachymetry assesses corneal thickness, and is an important measurement for many corneal diseases that affect corneal thickness distribution, such as ectatic disorders like KC

(Ramesh et al. 2017). Pachymetry has historically measured only central corneal thickness (CCT); however, developments in technology can produce a thickness map of the entire cornea (Li et al. 2006). OCT can be used for corneal pachymetry measurement by employing much faster scans of the eye's anterior segment, at 4,000 axial scans per second (Goldsmith et al. 2005; Radhakrishnan et al. 2001). AS-OCT can be performed with machines designed to perform posterior segment scans via a lens adapter (Shan et al. 2019), and these can produce pachymetry maps or single images of the entire anterior chamber angle. However, detailed tomographic mapping of the posterior cornea requires a distinct machine with swept source/Fourier domain capabilities to map epithelial thickness distribution (Li et al. 2012) and posterior corneal surface topography and cross-sectional images (Yip and Chan 2019).

Recent literature has suggested that using tomography (often optical coherence tomography, or OCT) in conjunction with topography improves sensitivity and specificity of detection of corneal ectasia (Belin et al. 2014; Cavas-Martinez et al. 2016; Gomes et al. 2016). Experts have agreed that tomography is the best method to diagnose KC in its early stages as abnormalities in posterior corneal elevation are required to diagnose mild or subclinical KC (Gomes et al. 2015). However, there are limitations to using tomography machines including their high price, large size, power requirement, and the need for skilled technicians to acquire and analyze images (Chopra et al. 2021), and as such they are not yet ubiquitous in optometric practice (Barrett and Loughman 2018; Jindal et al. 2019; Myint et al. 2011; Stein et al. 2012).

1.1.3.3 Complexity of Detection of KC

KC results in irregular corneal thickness distribution and steepness. Corneal thinning results in a decrease in corneal volume, which is a hallmark sign of KC (Toprak et al. 2021). Detection of KC is based on corneal imaging methods including topography, tomography, and pachymetry. Currently, the gold standard for detection of early KC is tomography (Anitha et al. 2021; Gomes et al. 2015). Topography is more common and thus often relied on to flag for suspicion (Ambrósio et al. 2003; Cavas-Martinez et al. 2016; Salomão et al. 2018; Santodomingo-Rubido et al. 2022). However, the use of a single value or parameter to diagnose KC is not sufficient (Santodomingo-Rubido et al. 2022); abnormal posterior ectasia, abnormal corneal thickness distribution, and clinical non-inflammatory corneal thinning must be present to diagnose KC (Belin et al. 2022; Gomes et al. 2015) and some of these more subtle corneal changes are better detected via tomography (Gomes et al. 2015; Hashem et al. 2023; Omar et al. 2019; Salomão et al. 2018). KC is a diagnosis of exclusion and must be distinguished from other ectatic disorders such as pellucid marginal degeneration (PMD), Terrien marginal degeneration (TMCD), brittle cornea syndrome, and keratoglobus (KG) (Anitha et al. 2021).

In a case study of five children who were diagnosed with anisometropic meridional amblyopia, then referred after six to eight months of patching treatment with no improvement, two were observed to have biomicroscopic signs of KC (Vogt's striae and ectasia). All patients were subsequently diagnosed with KC without underlying amblyopia, and all were correctable to 20/20 with CL treatment (Arora and Lohchab 2019). This case

study demonstrates the importance of accurate detection of KC, the possibility of misdiagnosing KC as meridional amblyopia, and potential for visual improvement once the correct treatment was administered.

1.1.3.4 Nomenclature and Classification of KC

The nomenclature and categorization of early KC is contested, with multiple terms in use, including forme fruste, KC suspect, and preclinical (or subclinical) KC (Shi 2016). Generally, preclinical KC is defined as a cornea with no detectable abnormalities upon slit lamp examination, but inferior corneal steepening or asymmetry with unaffected vision. One of the first clinically detectable signs of KC includes changes to the posterior corneal surface, with the ratio of anterior and posterior corneal surface area significantly decreased in KC (Santodomingo-Rubido et al. 2022).

Various terms are in use to describe the early stages of KC, and often these get interchanged or used incorrectly, adding to difficulty performing research in KC and confusion regarding stage or severity. Names for the earliest stages of KC include forme fruste KC (FFKC), KC suspect, and preclinical or subclinical KC. FFKC was defined by Amsler, later modified by Klyce, and is now agreed to refer to a patient's fellow eye that does not exhibit clinical signs (such as Vogt's striae) or topographic signs (such as skewed bowtie astigmatism) with manifest KC in the other eye (Amsler 1946; Klyce 2009; Shi 2016). KC suspect has been defined in various ways, including the following (Shi 2016): a cornea with specific topographic changes (abnormal steepening often inferiorly, or an asymmetrical or skewed bowtie) and no KC in the fellow eye (Klyce 2009); the fellow eye of a KC eye without slit

lamp findings (Waring 1993), which aligns with the FFKC definition; and only asymmetric bowtie with skewed radial axis and no clinical findings (Li et al. 2009), which emphasizes the role of the IS and SRAX indices and whose definition aligns with subclinical KC. Subclinical KC has also been defined in several ways (Shi 2016), such as the fellow eye of one with manifest KC and specific features including no keratometric, retinoscopic, or biomicroscopic signs of KC, asymmetry or skewed bowtie pattern on topography, and no history of surgery, trauma, or contact lens wear (de Sanctis et al. 2008; de Sanctis et al. 2013; Uçakhan et al. 2011). It has also been defined by the presence of major and minor criteria, with major criteria being Vogt's striae or Fleischer's ring extending at least 2mm, SRAX index >20º, KPI >30%, KSI >30%, and abnormal KCI; and minor criteria being asymmetric bow-tie without SRAX, inferior steepening, KSI 15-30%, and KPI 23-30%; with subclinical KC being present if one major or two minor criteria were met (Jafarinasab et al. 2015). Subclinical KC is also used in a more vague sense to include both FFKC and KC suspect (Shi 2016).

While FFKC does have an agreed-upon definition, subclinical KC and KC suspect have much less clear definitions and are often used interchangeably to refer to the fellow eye of one with manifest KC with some identifiable feature KC but not severe enough to be classified as manifest KC (Shi 2016). This introduces many problems into the field of KC research and management, as the definition of the term used may differ from one study or clinician to another, and guidelines regarding management of each level of severity cannot be established.

The classification of KC severity is challenging because the time course for development of signs and symptoms as well as their association with disease severity are extremely variable (Santodomingo-Rubido et al. 2022). KC severity can range widely - very early preclinical stages include no visible biomicroscopic signs, normal topography, or a mild amount of refractive astigmatism. Extremely severe stages may include corneal scarring, perforation, extreme corneal thinning (as low as 200 μm), or large amounts of irregular astigmatism that may not be measurable via refraction (Gomes et al. 2015; Krumeich et al. 1998).

There are a number of existing proposed classification systems. The first proposed KC classification system was the Amsler-Krumeich, which was originally proposed by Amsler in 1947 and was based on keratometry and optical pachymetry, and as such accounted for central anterior curvature and apical thickness (Belin et al. 2020). It was later modified to include refractive error components myopia and astigmatism, as well as clinical findings including scarring and perforation, and is divided into stages I-IV (Krumeich et al. 1998). Each stage includes progressively increased amounts of myopia/astigmatism, steeper cornea, thinner pachymetry, and more severe clinical findings. This system was in place when KC was only managed with corneal RGP contact lenses and penetrating keratoplasty, but advances in imaging now allow for much earlier detection and management (Belin et al. 2020).

The Belin ABCD classification system was proposed in 2016 in order to address additional corneal characteristics of the posterior corneal surface and visual acuity (Belin et al. 2020). The four characteristics include anterior and posterior radius of curvature at thinnest location,

thinnest pachymetry, and visual acuity. Each characteristic is ranked from zero to five, and does not produce a single final value but rather describes each characteristic. It has also been developed to produce a depiction of progression as eight past exams can be displayed and compared. KC is a complex disease with many different effects manifested, and this system intended to address the requirements set out by the 2015 global consensus on keratoconus and ectatic diseases (Gomes et al. 2015) including corneal thinning, anterior and posterior steepening, and rate of change of corneal thickness, as well as advising clinicians to intervene before vision loss rather than managing once loss has already occurred (Belin et al. 2020). It is commonly displayed on tomography result printouts, but is not universally accepted as it fails to consider important disease features including asymmetry of corneal shape, any clinical findings such as striae or scarring, and corneal aberrations.

Other classification schemes include one published in 2013 by Sandali et al. that employed AS-OCT and proposed 5 stages of KC based on corneal morphological changes, but did not address anterior corneal shape changes, and this detailed level of imaging is not always accessible, so is not a good substitute for classification systems that describe the anterior corneal shape. Rather, these corneal micro-architectural features should be considered in addition to more easily measurable features. The Alió and Shabayek classification system essentially modified the Amsler-Krumeich by adding coma-like corneal aberrations (Alió and Shabayek 2006). The KISA% index is described earlier in this thesis and was adapted into the expanded KISA% index, which added tomographic information to the KISA% index which describes only topography (Steinberg et al. 2015). The KC severity scale (KSS), used in the CLEK study (Zadnik et al. 1998), was proposed as a KC severity grading that could be

automated and takes into account corneal topographic and aberrometric information along with clinical findings and manual interpretation of a topography map to produce an overall number indicating presence, suspicion, or severity of KC, also requiring decision-making and interpretation from the clinician.

Due to the different bases for the different classification schemes, they are appropriate for use in different scenarios, and one universal classification has not been agreed on (Giannaccare et al. 2021; Gomes et al. 2015).

1.1.4 Management

KC management centers on visual rehabilitation with contact lenses, often corneal rigid gas permeable (RGP), multicurve, or scleral RGP lenses (Anitha et al. 2021). Collagen crosslinking (CXL) is a procedure that is used to slow and stabilize the progression of KC by employing riboflavin drops and UV-A light which produces reactive oxygen species (ROS) that increase cross-linking between prostaglandins and collagen in the cornea, ultimately increasing corneal rigidity after the procedure (Anitha et al. 2021). CXL is generally safe and effective, and if patients' eyes are incompatible with CLs, may be required (Anitha et al. 2021). Classically the epithelium is removed via debridement, known as "epi-off," to allow for better penetration of riboflavin and UV light (Nughays et al. 2025). A newer development in the procedure can be performed without epithelial debridement, known as transepithelial or "epi-on" intended to reduce risk of infection, pain, and recovery time, and literature is mixed regarding efficacy compared to epi-on (Nughays et al. 2025). CXL helps to halt or

slow progression of KC, and does not reverse the process (Buzzonetti et al. 2020) but may improve measures such as visual acuity, and Kmax (Wajnsztajn et al. 2022).

Differences exist between adult and pediatric KC in disease entity and management guidelines. The best nonsurgical pediatric KC management includes verbal guidance to avoid rubbing eyes, use of topical anti-allergy medicines, use of preservative-free lubricants, and wearing glasses or CLs (Gupta et al. 2022). Research into keratoconus has been increasing in the past three decades (Gomes et al. 2016), with the greatest focus on treatment, specifically CXL. However, there is not extensive coverage of pediatric keratoconus. A landmark study in pediatric eye disease is the MEPEDS study of 2009 which analyzed the prevalence and causes of various visual impairments, but keratoconus was not featured strongly in this study.

1.2 Astigmatism and Meridional Amblyopia

In KC, the most common visual consequences are myopia and irregular astigmatism (Buzzonetti et al. 2020), a refractive condition in which the primary axes are not 90º apart and which is not fully correctable with sphero-cylindrical lenses (Goggin et al. 2000). The bulging out of the cornea in KC contributes to the myopic shift, and the irregularity in the shape of the cone contributes to the irregular astigmatism. It is possible to minimize or correct the degree of irregular astigmatism that occurs in KC using corneal or scleral rigid contact lenses, in which the tear reservoir evens out the irregular optical surface (Anitha et al. 2021; Goggin et al. 2000).

Amblyopia is a developmental disorder of vision in which the cortical connections between the eyes and the brain are not able to fully develop, and as such the amblyopic eye is not

correctable to 20/20 in adulthood. There is a “critical period” during which treatment can allow the cortical connections to form and vision to develop to normalcy; the consensus around the upper age limit for this period is contested, though, but is generally agreed to be between ages 7-10 (PEDIG 2005). Amblyopia can develop due to refractive error, strabismus, or form deprivation, or some combination of these factors (PEDIG 2002).

Amblyopia can be treated if addressed during the critical period, although some practitioners argue the existence of neural plasticity beyond this period (Astle et al. 2011; Levi 2005). Common treatments include patching or occlusion of the better-seeing eye in order to force use of the amblyopic eye and encourage development of cortical connections. The first-line treatment for refractive amblyopia is refractive error correction, though in anisometropic amblyopia, a concurrent treatment of patching or some other pharmacological treatment is often required (Cotter 2006).

Meridional amblyopia refers to orientation-dependent deficits in vision secondary to uncorrected astigmatism during the critical period of visual development due to irreversible neural adaptation even if the astigmatism reduces through emmetropization (Deshpande et al. 2018). The degree of reduction in visual acuity corresponds to the magnitude of astigmatism, with oblique orientation being the most amblyogenic and difficult to manage.

1.3 Specific Aims

In general, the literature regarding pediatric keratoconus is sparse, and most important papers or studies discussing pediatric eye disease do not feature KC strongly, if at all. Though KC is fairly uncommon in many parts of the US, knowing details about the disease process and

how to treat it is vital to helping those patients who do present with it. There is widespread agreement that detecting early or subclinical KC is much more difficult than advanced KC (Arora and Lohchab 2019; Gomes et al. 2015), which that delayed diagnosis of KC might be common, allowing disease progression to a more severe stage ultimately requiring much more invasive treatment including corneal graft surgery.

A pilot study was performed (Borle et al. 2022) which analyzed whether there was a significant difference between groups of high cyl (at least 3.5D) and low cyl (less than 3.5D) regarding prevalence of KC suspects as determined by their KPI. It was found that the relationship between these two categories of meridional amblyogenic risk factors and the presence or absence of early KC was not significant. This was surprising; given the small sample size, the current study continued this investigation on a larger scale and introduced measurement of additional data points relevant to KC diagnosis including pachymetry and corneal aberrations.

The overall aim of this study is to identify characteristics that are more strongly associated with early KC, or that are good predictors of KC development or progression, and are detectable with devices and methods more easily accessible to primary care optometrists, and to provide practitioners with guidelines about when pediatric patients should be evaluated for KC. This was addressed with three main goals:

Goal 1: Determine differences between pediatric subjects with low versus high amounts of refractive astigmatism and whether prevalence of KC suspicion was correlated.

Goal 2: Determine one or more characteristic(s) that reliably predict KC suspicion based on KPI.

Goal 3: Determine differences between pediatric subjects with astigmatism who were flagged as KC suspects based on KPI and those who were not flagged.

It was hypothesized that subjects with higher refractive cyl would be more likely to be KC suspects as well as display more extreme corneal metrics of steepness and asymmetry correlating with higher KPI. It was also hypothesized that some corneal characteristic(s) would correlate well with KPI and be good predictors of this value.

2. Methods

2.1 Subjects & Recruitment

Subjects were recruited for this study from the Charles River Community Health Center in Brighton, MA during the course of comprehensive eye exams. Inclusion criteria were children between 5 and 18 years of age (average age of subjects was 10.66 ± 3.62 years), and at least 1D of astigmatism, or cylindrical refractive error (cyl) in both eyes. Exclusion criteria included a previous diagnosis of corneal disease including ectasia, opacification, trauma, or transplant. No exclusions were made on the basis of visual acuity, or a prior diagnosis of amblyopia.

In this study KC suspects were defined by their KPI, using a cutoff of 23% as established in prior studies (Maeda et al. 1994; Shi 2016). Subjects with a KPI ≥ 23% as measured by the Topcon CA-800 were referred to a pediatric corneal specialist for tomography and confirmation of diagnosis, and potential further management such as corneal cross-linking. Unfortunately, patient retention following referrals was limited. Typically, referrals to pediatric specialists were requested within about 3 months.

The study was approved by the Institutional Review Board of the New England College of Optometry and conforms to the declaration of Helsinki. Subjects were recruited during pediatric comprehensive eye exams, and proper parental consent was obtained prior to data collection.

2.2 Procedures

A comprehensive eye exam was performed in which a complete case history was gathered including birth history, personal and family history of systemic or ocular diseases, and history of ocular trauma or infection; testing of visual acuity, uncorrected and corrected if applicable; ocular alignment via cover test; cycloplegic retinoscopy; and thorough ocular health assessment including anterior segment biomicroscopic examination and dilated fundus exam.

At the end of their comprehensive eye exam, the subjects with ≥1D astigmatism had topography measurements taken by the Topcon Corneal Analyzer CA-800, followed by pachymetry measurements using the Zeiss Cirrus HD-OCT 500. Several topographic indices were captured including Sim K values, K cyl, AK, AGC, SD, SI, and SAI (see background for descriptions). Aberrations measured in this study were all derived from the corneal shape and included primary astigmatism, described by Topcon as a depiction of how the wavefront is affected by topography along axes 90º apart (Topcon 2024), but no published information is available detailing the exact calculation of this term; spherical, coma, higher order, and total aberrations, all reported as RMS in µm.

Astigmatism aberrations depict how the subject's wavefront is affected by their topography along axes 90º apart; spherical aberration measures how the wavefront is altered by the cornea near the pupil margin compared to the center of the cornea; coma indicates how the wavefront is altered by opposite hemispheres of the cornea; and Topcon describes the HOA

term as a combination of all other aberrations not included in the other measurements (Topcon 2024), meaning it includes an RMS value of all aberrations 3rd order and above.

From the topographer's keratometry data, K values and amount of K cyl were recorded and steepest corneal location was determined from the resulting steepness map and corresponding K-readings. This was used to guide measurement of corneal thickness at the steepest corneal location, in addition to central and inferior locations.

As study data was collected during subjects' comprehensive eye exams, differences in methods of pachymetry measurements were unavoidable and are a recognized weakness in this study. Subjects from a pilot study were included in analysis, and pachymetry was not yet being measured, so some subjects did not have pachymetry values. Once recruitment began for this study, pachymetry was measured using the OCT by manually selecting the central, steepest, and inferior locations and capturing individual scans of each corneal region and measuring thickness at each. Partway through data collection, the machine capabilities were updated to capture full-corneal pachymetry maps from which the correct value could be read by matching the measured point on the map rather than measuring at each point of interest individually. This introduced variability in how data was collected and should be noted when discussing pachymetry results.

Various additional data points acquired through the exam were included in analysis, including past and current spectacle Rx, BCVA, and any relevant anterior and posterior segment findings such as Fleischer ring, Munson sign, oil droplet reflex, scissoring reflex on

retinoscopy, corneal scarring, optic disc appearance, C/D ratio, macula, and peripheral findings.

2.3 Statistical Analysis

The present study was a continuation of the pilot study by Borle et al., and data were pooled for analysis. Prior to beginning the study, using the R studio package “pwr” it was determined that a minimum of 80 subjects (160 eyes) was needed to achieve a power of 0.75 and two-sided alpha level (type 1 error) of 0.05, for a small (Cohen’s d = 0.3) effect size (Blanca et al. 2023).

Analysis in this study was conducted using R studio. Converting refractive error to vector components was achieved using a simple command that reads the sphere, cylinder, and axis values and performs mathematical and geometric analysis to return a data frame containing the components M, J0, and J45.

Goal 1: Because it was hypothesized that there would be differences between subjects with high and low amounts of astigmatism, the cohort was split into two groups - high cyl (at least 3.50D), which included 43 eyes of 27 subjects, and low cyl (less than 3.50D), which included 121 eyes of 65 subjects. A Welch’s 2-sample t-test was used to determine significant differences between the two groups and the p-values were adjusted using the false discovery rate (FDR) method, which states the expected proportion of false positives among all positive cases identified. It is recommended to adjust p-values when performing repeated analyses on the same data, and FDR is considered the best adjustment method because it minimizes both false positives and negatives (Jafari and Ansari-Pour 2019).

Goal 2: Additionally, it was hypothesized that some corneal characteristic or metric would be correlated with presence of KC as identified by the index KPI. Linear modeling was performed to determine which data points were good predictors of KPI as determined in this study. Linear models depict how well variable y is predicted by each continuous variable x, with each model containing descriptors indicating how successful the model is. A p-value describes the model's significance, and an r-squared value indicates goodness of fit of the model, ranging from 0-1 with 1 being 100% predictive value. The most significant models were chosen first based on whether they had significant p-values of $p < 0.05$, as was used elsewhere in this study to determine significance, then based on r-squared values >0.15 in order to compare goodness of fit among statistically significant linear models.

A "good" r-squared value depends on what is being studied, with values being considered significant ranging from 0.1 to 0.9 depending on the field of study, such as psychology, finance, and chemistry. The medical field does not have a standard acceptable value and arbitrary bounds are often used; however, an r-squared of >0.15-0.20 may be considered meaningful in clinical studies, particularly in the context of multifactorial conditions (Gupta et al. 2024).

The use of linear modeling also allows for multivariate analysis, which allows the researcher to consider whether a certain combination of data points may hold higher predictive power. There is a tradeoff in multivariate analysis, however, with models including more parameters requiring penalties for additional parameters. This design allows for valid analysis of this dataset, with the possibility of identifying variables with good predictive power for KPI.

It is important to note that pachymetry was not performed for the 31 subjects whose data were collected during the pilot study. Additionally, certain indices were not obtained for two participants due to error in either measurement or calculation by the corneal topographer during the assessment of corneal shape. In analyzing the data to create these models, only subjects' eyes that contained all data points were included, so all subjects from the pilot study were excluded from the creation of linear models, with 59 eyes included in this final analysis. This sample size was lower than the target determined by the a priori power analysis, so this analysis likely was underpowered to detect the expected effect.

Because the sample size was relatively small and was further decreased when excluding incomplete datasets, bootstrapping was performed. Bootstrapping involves taking an existing data set and randomly resampling from it to create a much larger dataset with similar composition. In this study, the linear models were bootstrapped to produce 2,000 samples and determine 95% confidence intervals.

Goal 3: In order to identify differences between eyes with suspected KC and those without, subjects were divided again into two groups - eyes identified as KC suspects based on KPI, which consisted of 15 eyes of 12 subjects, and eyes not identified as KC suspects, which consisted of 149 eyes of 70 subjects. Data was analyzed similarly to the groups of low and high cyl, with a Welch's 2-sample t-test to determine significant differences between the two groups. Again, the p-values were adjusted using the FDR method.

3. Results

3.1 General Results

Subjects' eyes were analyzed individually; a total of 82 subjects (n = 164 eyes) were enrolled between March 2023 and November 2024. There were 33 (40.2%) female subjects and 49 (59.8%) male subjects. 41 subjects were Hispanic (50.0%), 3 were Indian/South Asian (3.7%), 2 were Black (2.4%), 2 were White (2.4%), and 3 were another race/ethnicity (3.7%). The average sphere refractive error was +0.69 ± 2.59D, with average cyl -2.72 ± 1.25D. 12 subjects (14.6%) were determined to have a KPI ≥23%. Of the 12 subjects with KPI ≥23%, there were 3 (3.7%) confirmed cases of keratoconus and 2 (2.4%) subjects were determined to not have keratoconus. Unfortunately, 7 patients were lost to follow-up and keratoconus status could not be determined. Two eyes with KC suspicion had scissoring reflex on retinoscopy, and none of the non-suspects had a scissoring reflex. Descriptive statistics for the entire cohort are available in Appendix I, and all box plots depict variables with statistically significant differences between groups with 95% confidence intervals.

3.2 Low and High Cyl Groups

Subjects were categorized in this study as high cyl (≥ 3.50D) or low cyl (< 3.50D) based upon the amount of astigmatism identified during cycloplegic retinoscopy. The high cyl group consisted of 43 eyes (26.2%) of 27 subjects, with a mean cyl value of -4.42 ± 0.89D (Figure 1). This group had 21 (77.8%) males and 6 (22.2%) females. The low cyl group consisted of 121 eyes (73.8%) of 65 subjects, with a mean cyl value of -2.12 ± 0.66D (Figure

1). This group had 35 (53.8%) males and 30 (46.2%) females. A summary of the results of analysis is available in Appendix II.

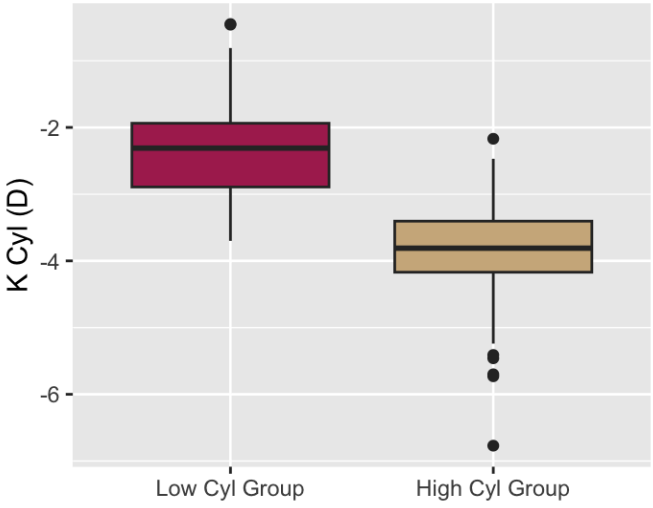

Figure 1: Average K Cyl in Low and High Cyl Groups

3.2.1 Topographic Indices - Steep K, SAI

In this study the high cyl group was found to have steeper steep K values than the low cyl group (45.06 ± 1.70D, low cyl 44.11 ± 1.93D, $p < 0.01$, Figure 2).

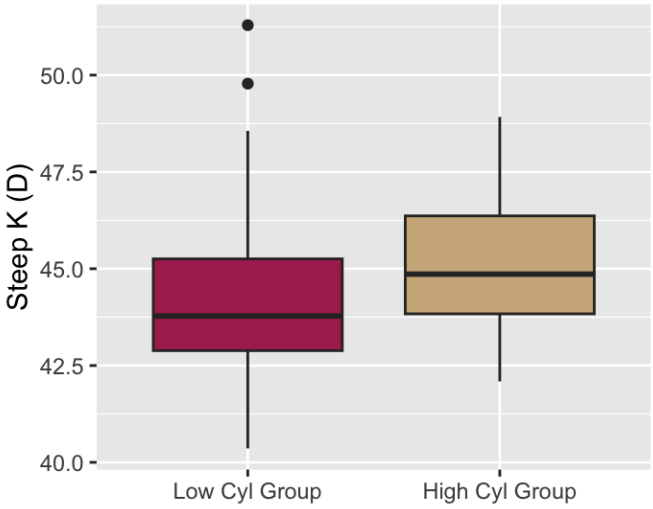

Figure 2: Average Average Steep K in Low and High Cyl Groups

The high cyl group had more surface asymmetry than the low cyl group, as SAI was statistically significantly different (high cyl 0.61 ± 0.56, low cyl 0.42 ± 0.33, $p < 0.05$, Figure 3). The SI index was not found to be different between these groups ($p = 0.273$).

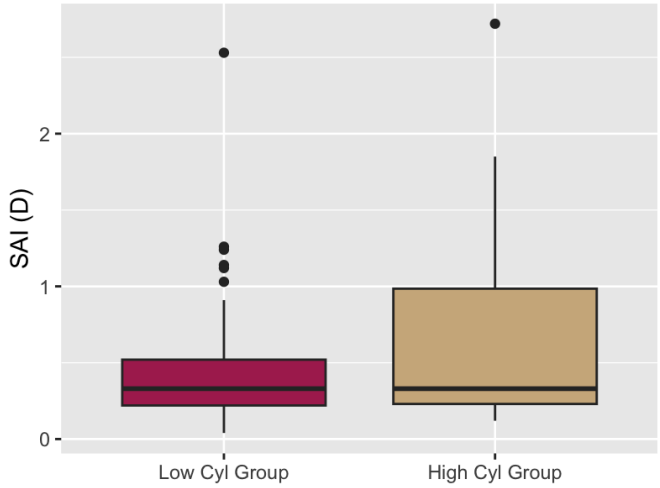

Figure 3: Average SAI in Low and High Cyl Groups

3.2.2 Aberrations

Statistically significant differences were found between the groups for total aberrations (high cyl 4.45 ± 0.98µm, low cyl 2.92 ± 1.39µm, $p < 0.01$, Figure 4), and astigmatism aberrations (high cyl 3.79 ± 0.84µm, low cyl 2.37 ± 1.07µm, $p < 0.01$, Figure 5).

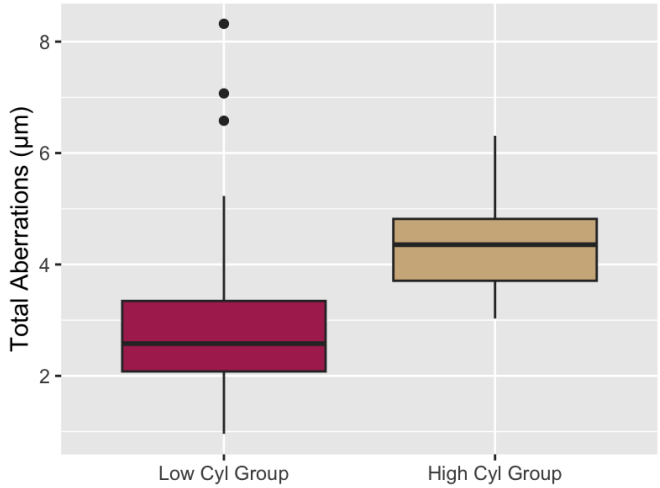

Figure 4: Average Total Aberrations in Low and High Cyl Groups

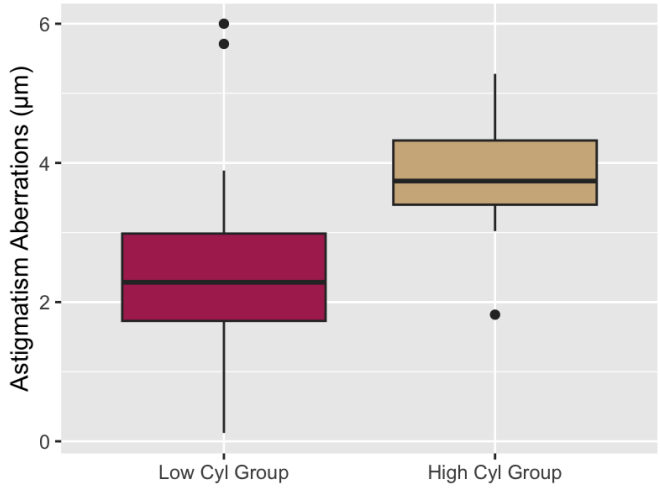

Figure 5: Average Astigmatism Aberrations in Low and High Cyl Groups

3.2.3 Refractive Vector Components

M was found to be statistically significantly more negative in the high cyl group than the low cyl group (high cyl -1.65 ± 0.97D, low cyl -0.79 ± 1.37D, $p < 0.01$, Figure 6). J0 was also found to differ significantly between the two groups (high cyl 2.15 ± 0.45D, low cyl 0.99 ± 0.37D, $p < 0.01$, Figure 7).

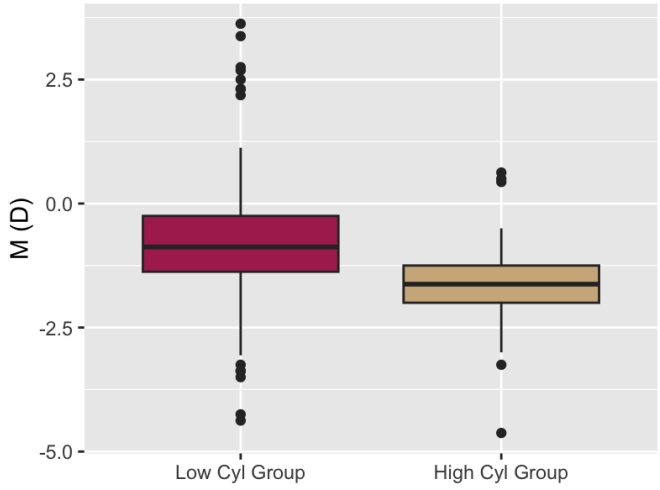

Figure 6: Average M in Low and High Cyl Groups

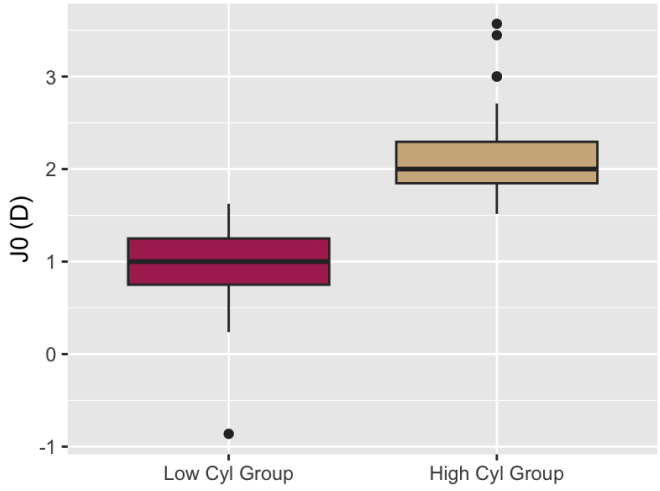

Figure 7: Average J0 in Low and High Cyl Groups

The entire cohort consisted of a mix of myopes and hyperopes, with 23 compound hyperopic astigmatic (CHA) eyes (14%), 1 simple hyperopic astigmatic eye (0.6%), 79 mixed astigmatic eyes (48%), 22 simple myopic astigmatic eyes (13%), and 39 compound myopic astigmatic (CMA) eyes (24%). The high cyl group consisted of 3 CHA eyes (7%), 31 mixed astigmatic eyes (72%), 3 simple myopic astigmatic eyes (7%), and 6 CMA eyes (14%). The

low cyl group consisted of 22 CHA eyes (18%), 1 simple hyperopic astigmatic eye (0.8%), 46 mixed astigmatic eyes (38%), 19 simple myopic astigmatic eyes (16%), and 33 CMA eyes (27%).

3.2.4 Pachymetry

Since pachymetry (measured via OCT) was not introduced until after the pilot study was completed, the 31 subjects without these values were excluded from this portion of analysis, leaving 59 subjects (118 eyes) with pachymetry results. Due to the inconsistencies in data collection, as well as the smaller sample size compared to the other data points collected, pachymetry results were ultimately excluded from the findings of this thesis.

3.3 KPI and Linear Modeling

Figure 8 shows a barplot to visualize adjusted r-squared values. According to p-values and adjusted r-squared values the best overall model used the parameters Age, Steep K, AK, AGC, SD, Kc, SI, SAI, K cyl, M, J0, J45, Total Aberrations, Astigmatism Aberrations, SA, Coma, HOA ($r^2 = 0.418$); all parameters aside from pachymetry values. The second-highest r-squared value, 0.374, corresponded to a model with three components - Age, AGC, and SD. When attempting to limit the amount of parameters included in a model, no improvement to the best-performing model could be made by including more than four but fewer than all the parameters. A table with descriptions of all models is available in Appendix III.

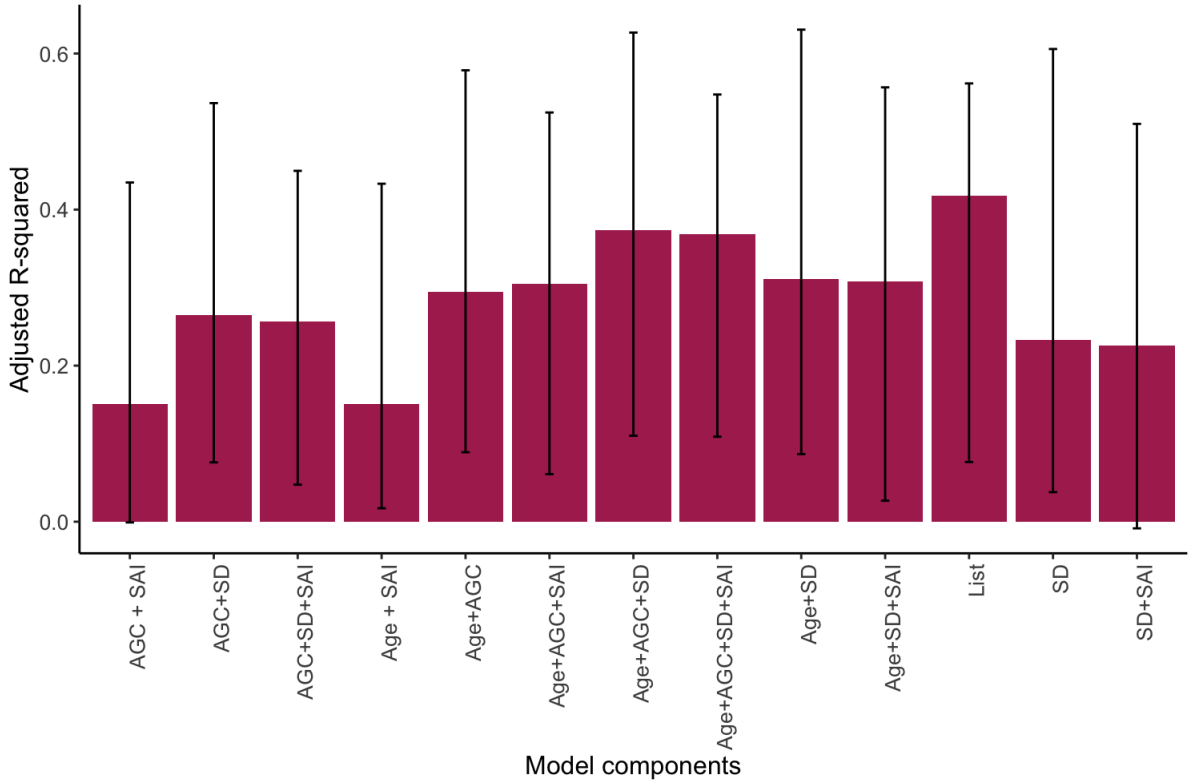

Figure 8: Significant Linear Models with Bootstrapped 95% CIs

Note: "List" contains model parameters Age, Steep K, AK, AGC, SD, Kc, SI, SAI, K cyl, M, J0, J45, Total Aberrations, Astigmatism Aberrations, SA, Coma, HOA

However, an interesting finding of this analysis was that all the models fall within 95% confidence intervals of one another - the bootstrap produced 2,000 replications and was able to provide confidence intervals, and it can be seen in Figure 8 that these confidence intervals are very wide, enough so that each model falls within the intervals of the others.

Other than a model containing age and all topographic, refractive, and aberrometric parameters, the models with the highest r-squared values included the indices age, AGC, SD, and SAI in varying combinations.

3.4 KC Suspects vs. Non-Suspects by KPI

Subjects were categorized as KC suspects with KPI ≥23% and non-suspects with KPI <23%. The KC suspect eyes group consisted of 15 eyes (9.1%) of 12 subjects, with a mean cyl value of -3.07 ± 1.36D and a mean age of 13.07 ± 3.40 years. Three subjects were flagged as KC suspects in both eyes. The non-KC suspect eyes group consisted of 149 eyes (90.9%) of 70 subjects, with a mean cyl value of -2.69 ± 1.24D and a mean age of 10.42 ± 3.50 years. The KC suspect group had 8 (66.7%) males and 4 (33.3%) females, and the non-suspect group had 41 (58.6%) males and 29 (41.4%) females. The Welch's 2 sample t-test found no statistically significant differences between the groups for cyl, AK, AGC, SD, Kc, spherical aberration, coma, higher order aberrations, J0, or J45.

3.4.1 Refractive Vector Components

Spherical equivalent refractive error was found to be more negative among the KC suspect group (KC suspects -1.38 ± 1.00D, non-KC suspects -0.60 ± 2.64D, $p < 0.05$, Figure 9). The power vector M, representing spherical equivalent in its orthogonal form, was found to be more negative among the KC suspect group (KC suspects -1.46 ± 0.65D, non-KC suspects -0.97 ± 1.38D, $p < 0.05$, Figure 10). No differences were found between groups for J0 ($p = 0.271$) or J45 ($p = 0.837$).

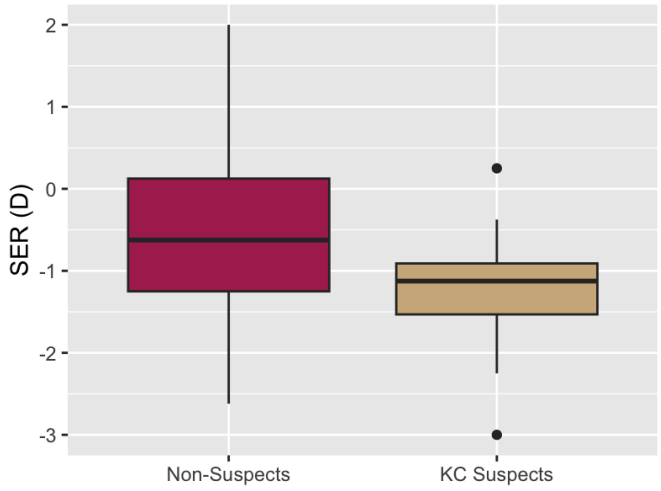

Figure 9: Average SE in KC Suspects and Non-suspect Groups

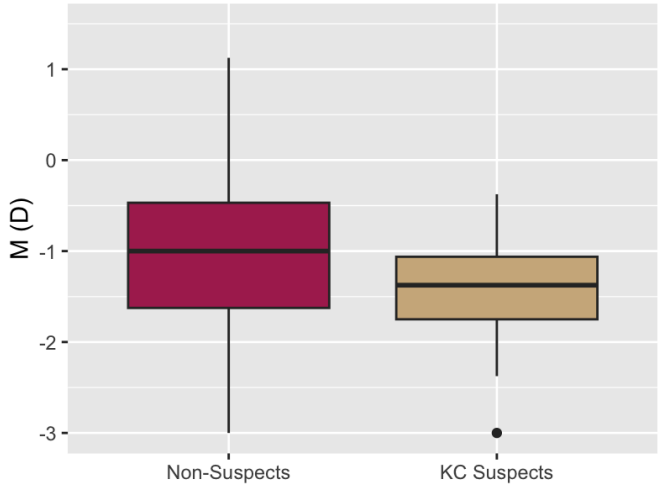

Figure 10: Average M in KC Suspects and Non-suspect Groups

As described earlier, when performing research related to refractive error, it is necessary to convert sphere, cylinder, and axis into power vectors that can be analyzed independently. Therefore, this finding should not be regarded as a statistical predictor of KC. However, as M is an orthogonal vector, it may be considered in statistical analysis of refractive error.

The KC suspects included 0 CHA or simple hyperopic astigmatic eyes, 7 mixed astigmatic eyes (47%), 5 simple myopic astigmatic eyes (33%), and 3 CMA eyes (20%). Non-KC suspects consisted of 25 CHA eyes (17%), 1 simple hyperopic astigmatic eye (0.7%), 70 mixed astigmatic eyes (47%), 17 simple myopic astigmatic eyes (11%), and 36 CMA eyes (24%). A higher percentage of KC suspect eyes were simple myopic astigmatic, and while a higher percentage of non KC suspect eyes had CMA, the percentages were very similar and the sample size was much smaller for the suspect group. Overall the spherical vector component M was significantly more negative in KC suspects than non-suspects.

3.4.2 Topographic Indices - K cyl, Steep K, SI, SAI

K cyl was found to be more negative among the KC suspect group (KC suspects -3.58 ± 1.32D, non-KC suspects -2.70 ± 0.93D, $p < 0.05$, Figure 11).

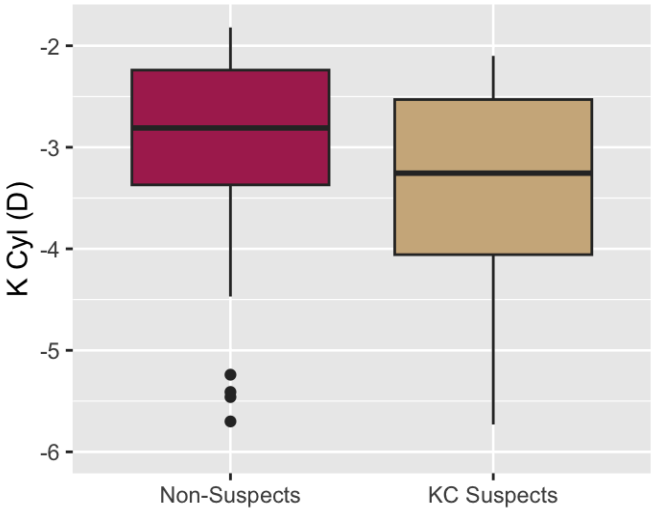

Figure 11: Average K cyl in KC Suspects and Non-suspect Groups

Corneal steep K was found to be steeper in the KC suspect group (KC suspects 45.45 ± 2.03D, non-KC suspects 44.25 ± 1.88D, $p < 0.05$), Figure 12).

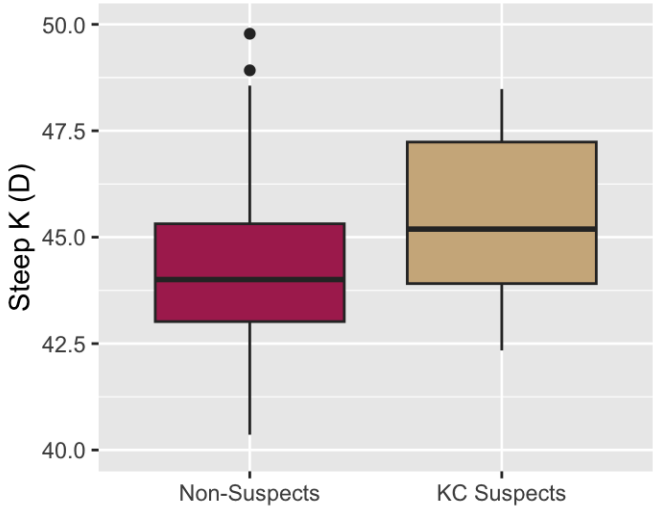

Figure 12: Average Steep K in KC Suspects and Non-suspect Groups

SI was found to be more negative among the KC suspect group (KC suspects -1.13 ± 1.27D, non-KC suspects -0.40 ± 0.72D, $p < 0.05$, Figure 13), indicating more inferior-superior asymmetry among patients suspected of KC.

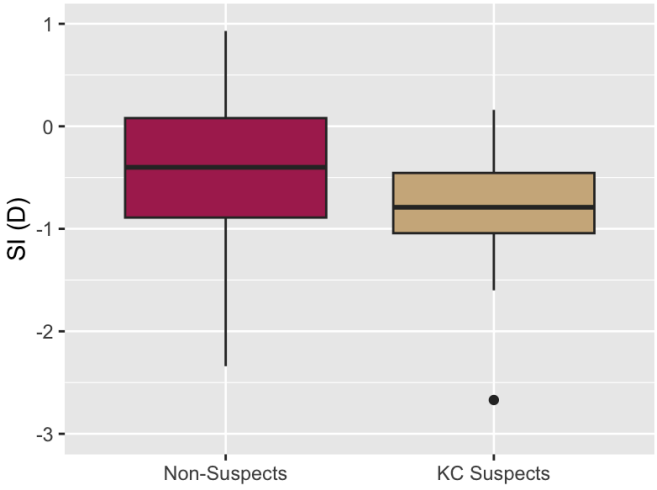

Figure 13: Average SI in KC Suspects and Non-suspect Groups

SAI was found to be higher among the KC suspect group (KC suspects 0.91 ± 0.87D, non-KC suspects 0.42 ± 0.30D, $p < 0.05$, Figure 14), indicating more corneal surface asymmetry among KC suspects.

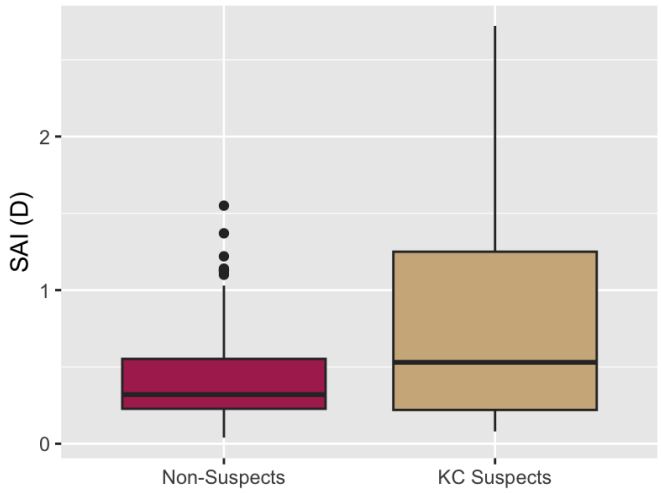

Figure 14: Average SAI in KC Suspects and Non-suspect Groups

3.4.3 Aberrations

Total aberrations were found to be greater among the KC suspect group (KC suspects 4.286 ± 1.352µm, non-KC suspects 3.088 ± 1.413µm, $p < 0.05$, Figure 15), as well as astigmatism aberrations (KC suspects 3.815 ± 1.471µm, non-KC suspects 2.495 ± 1.048µm, $p < 0.05$, Figure 16).

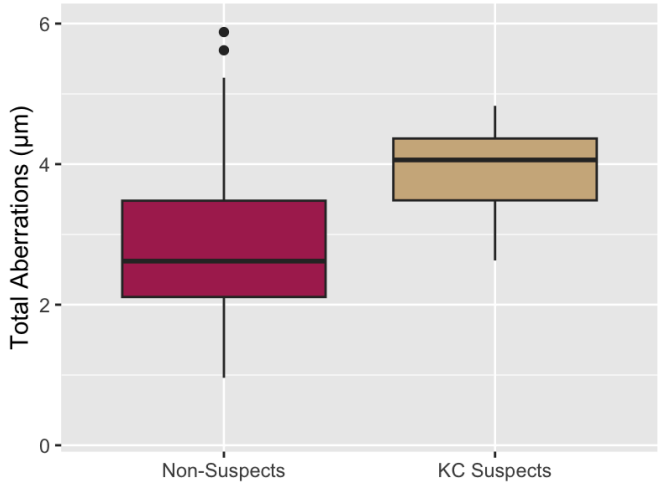

Figure 15: Average Total Aberrations in KC Suspects and Non-suspect Groups

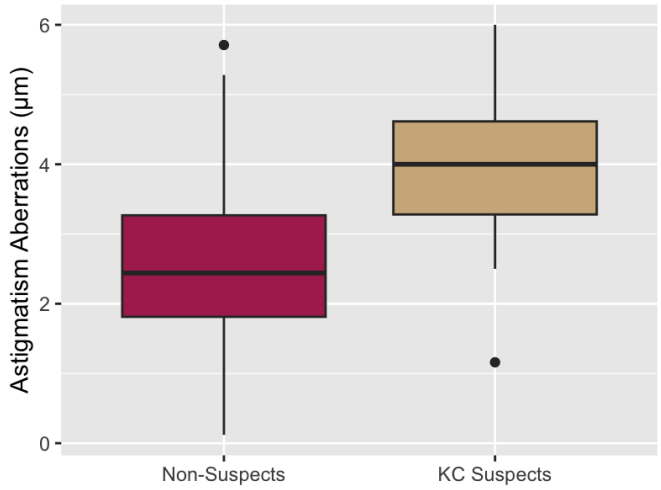

Figure 16: Average Astigmatism Aberrations in KC Suspects and Non-suspect Groups

3.4.4 Age

KC suspects (mean age 13.07 ± 3.41 years) were statistically significantly older than non-suspects (mean age 10.42 ± 3.56 years, $p < 0.05$, Figure 17), with age of KC suspects ranging from 7 to 18 years. This finding aligns with the results of the linear modeling that

found that age was a strong predictor of KPI, and agrees with what the literature predicts regarding pediatric patients developing KC closer to the age of puberty.

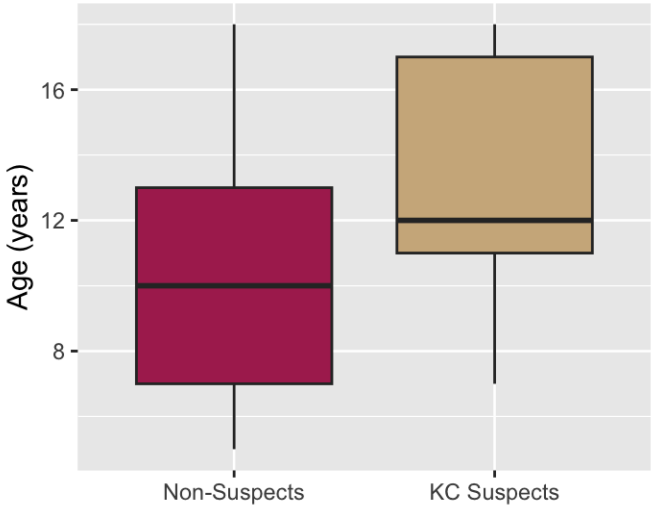

Figure 17: Average Age in KC Suspects and Non-suspect Groups

3.4.5 Summary of Results Analyzing by KPI

Altogether, subjects flagged as KC suspects tended to have a more negative M but not necessarily higher amounts of astigmatism based on J0 and J45, more steep and asymmetric corneas, increased aberrations, and were slightly older.

There were no significant differences between the KC suspects and non-suspects for several data points that were expected to exhibit differences, including topography indices AK, AGC, SD, and Kc, which describe maximum corneal steepness and rate of change of corneal curvature; as well as aberrations including spherical aberration, coma, and HOAs.

3.5 Summary of Overall Results

In this study, when dividing subjects into groups both by amounts of cyl and based on KPI, significant differences were found in K cyl, steep K, SAI, total aberrations, astigmatism aberrations, and M. J0 was significantly different in the cyl analysis but not KC suspects. SI and age were significantly different in the KC suspect analysis but not cyl analysis. Variables that were not found to be significant included AK, Kc, spherical aberration, coma, HOAs, and J45.

4. Discussion

This study investigated corneal characteristics of children with astigmatism of at least 1D who were flagged as KC suspects based on KPI ≥23% derived from topography in order to identify the presence of some measurement that could potentially flag or screen for early KC. In order to investigate this, subjects were recruited during comprehensive eye exams and corneal topography, aberrations measurement, and pachymetry were measured for those who met the inclusion criteria. Suspects identified in this study were referred to a pediatric specialist for confirmation of diagnosis.

This cross-sectional study allowed for analysis based on characteristics measured, as well as based on whether subjects were identified as KC suspects. Because the goal of the analysis was to identify differences between suspected KC eyes and non-suspect eyes, grouping subjects this way allowed for direct comparison.

4.1 Analysis When Grouping by Low and High Cyl

Subjects were categorized in this study as high or low cyl with these same categories based upon the amount of astigmatism identified during cycloplegic retinoscopy. This categorization was based on the hypothesis that higher amounts of cyl would correlate with increased incidence of KC suspicion, since literature supports that a common finding in KC is increased cyl (Buzzonetti et al. 2020; Gomes et al. 2015; Krumeich et al. 1998). It was also hypothesized that the group with higher refractive cyl would have more extreme corneal metrics of steepness and asymmetry correlating with higher KPI.

Because KC is associated with increased astigmatism and causes steepening and thinning of the cornea as well as aberrations (Anitha et al. 2021; Buzzonetti et al. 2020), it was expected that the higher cyl group would have more features typically associated with KC than the lower cyl group, including more corneal cyl, steeper corneal curvature and keratometry values, higher surface asymmetry, higher aberration values, and thinner pachymetry.

There was no significant difference in KC suspect incidence between the two groups, indicating that amount of cyl was not necessarily correlated with KC suspicion, as was hypothesized and consistent with the findings of Borle et al. The higher cyl group was found to have more corneal cyl, steeper K measurements, higher SAI, more total and astigmatism aberrations, more negative M, and higher J0. This was an interesting finding, since it is very common for clinicians to suspect KC based on the amount of cyl, and higher amounts of astigmatism are correlated with KC presence (Garcia-Ferrer et al. 2019; Gomes et al. 2015; Zhao et al. 2024).

4.1.1 Topographic Indices

In this study the high and low cyl groups had significantly different corneal cyl. This finding is expected and unsurprising - cycloplegic retinoscopy was used to determine the amount of refractive cyl in these pediatric patients, and typically identifies overall refractive astigmatism, the majority of which is due to corneal astigmatism as stated in Javal's rule, which is based on the assumption that internal (or lenticular) astigmatism is relatively constant in most people, -0.50D ATR, which has been validated in numerous studies (Read et al. 2007). This comparison is useful in confirming the validity of the data collected, but is not

useful in analyzing differences between the groups. Lenticular or irregular corneal astigmatism appear during retinoscopy as a scissoring reflex (Enaholo et al. 2025), and only two subjects in this study had irregular retinoscopy reflexes, both of whom were identified as KC suspects.

The high cyl group was also found to have steeper steep K values than the low cyl group. This finding is consistent with the hypothesis that the group with more astigmatism would have more extreme corneal characteristics including steeper corneas. Corneas with increased corneal cyl have steeper curvature by definition, so in addition to magnitude of corneal cyl, this finding confirms the validity of the data but does not aid in analyzing group differences and drawing conclusions.

The high cyl group had more surface asymmetry than the low cyl group, as SAI was higher in the high cyl group. SAI does not increase with regular astigmatism, rather with irregular variations in curvature or displaced steepening (Burns et al. 2004). Because higher SAI occurred in the high cyl group, this suggests that this group also had significantly higher rates of irregular astigmatism, which is correlated with KC disease presence and progression (Buzzonetti et al. 2020).

4.1.2 Refractive Error and Vector Components

While the proportion of myopic eyes was lower in the high cyl group, M was still significantly more negative. As the high cyl group necessarily consisted of subjects with higher amounts of astigmatism, this would make the overall spherical equivalent of refractive

error more negative. Again this result is not useful in analyzing differences between the groups as it is reflected in the way the groups were divided.

As the groups were divided based on the raw data value of cyl, J0 was expected to be significantly higher in the high cyl group, as was found. This finding, similar to both K cyl and steep K, is not very useful in analyzing differences between the groups. However, it is worth noting that there was no significant difference in the J45 component between the groups, indicating that in this cohort, subjects with higher overall astigmatism did not necessarily have oblique astigmatism.

4.1.3 Aberrations

It was expected that the higher cyl group would have higher incidence of KC suspects and thus more overall aberrations as well as specifically those normally associated with KC, including HOAs, spherical aberration (SA), and coma (Gobbe and Guillon 2005). Differences in astigmatism aberrations between groups split by amount of astigmatism were expected, as astigmatism aberrations are second order Zernike aberrations (along with defocus) that essentially describe refractive error normally compensated for with eyeglasses. The fact that no differences were found between the groups for the other types of aberrations, particularly those normally associated with KC, further indicates that dividing subjects based on astigmatism is not a valid indicator for higher suspicion of KC.

4.1.4 Summary of Findings When Analyzing by Amount of Astigmatism

The overall goal of this study was to provide evidence to support guidelines for clinicians in detection of KC in pediatric patients. The findings of this study indicate that while increased cyl is often found in KC, the amount of cyl at one point in time does not necessarily indicate suspicion for developing KC.

The fact that the amount of cyl was not a predictive factor in KC suspicion negates a commonly held belief among clinicians and suggests that amount of astigmatism should not necessarily be considered a major contributing factor to suspicion of early KC and the decision to screen for it. Further, when considering making a diagnosis of KC, more care should be taken to consider all information about the patient, rather than basing a decision on one finding.

Findings in the high cyl group directly reflect the fact that groups were delineated by amount of cyl - K cyl and steep K are directly related to cyl; SAI is an indicator that the corneal curvature is less spherical, which is also a feature of astigmatism; astigmatism aberrations are lower order aberrations that represent astigmatic refractive error, which is essentially another way of stating refractive error, albeit in terms of the optics of the eye as a system; J0 is also simply a restatement of the astigmatism by extracting the WTR/ATR component into vector format; and total aberrations would be expected to increase as astigmatic aberrations increased, considering that no other types of aberrations were found to be different.

There have been many proposed classifications of KC based on features including amount of induced refractive error (i.e., myopia or astigmatism), corneal steepness, corneal signs

including scarring and perforation, corneal thickness, and microarchitectural findings of the cornea identified with advanced imaging techniques such as anterior segment OCT (Krumeich et al. 1998; Sandali et al. 2013). No accepted classification system currently exists (Giannaccare et al. 2021; Gomes et al. 2015). Performing research in KC is complicated by the lack of agreed-upon classification, so in order to reach consensus on screening guidelines an adequate classification system of early or suspected KC stages is needed.

In this study, our first investigation dividing subjects into groups based on the amount of astigmatism did not yield significant results, and high cyl was not predictive of KC. Advancing KC is typically associated with increased myopia (Krumeich et al. 1998), but no literature consensus exists regarding typical refractive features of early/subclinical KC (Castro-Luna and Perez-Rueda 2020; Naderan et al. 2018; Reddy et al. 2014). A single measurement of refractive cyl in one eye likely should not be included in overall KC classification due to conflicting results and lack of strong evidence.

4.2 KPI and Linear Modeling

Using linear modeling allows for exploration of correlations between variables and predictive power of these variables. This format of analysis was used because a goal of this study was to identify a data point that is highly correlated with development of KC in order to recommend that clinicians place more focus on it when considering screening for KC. Within the equipment available for this study, the ultimate best indicator for suspicion of KC is the index KPI. This value was considered the dependent variable in this analysis, with all other numerical variables being considered as possible predictors.

According to Topcon, whose technology was used in this study, KPI is calculated based on the indices AK, AGC, and SI (Topcon 2024). Maeda et al. have also used a multivariate index called KPI calculated from a different set of eight indices: SimK1, SimK2, SAI, DSI, OSI, CSI, IAI, and AA.

The definition of KPI per Topcon and that used in the older paper by Maeda et al. differ greatly, which exemplifies why it is difficult to discuss standardized research in the field of topography and KC. Multivariate indices that are intended to predict KC such as KPI are typically dependent on the specific topographer, and not all indices described in certain definitions are produced by all topographers - many of the indices described in the alternate calculation of KPI by Maeda et al. are not produced by the topographer used in this study. Therefore, it is much more difficult to comment directly on how any singular data point might influence KPI. This issue gave rise to the purpose of this study, which is to provide clearer guidelines regarding the detection of KC suspects and which clinical features to pay attention to.

KPI is a widely accepted indicator of KC suspicion, with a reported sensitivity of 68% and a specificity of 99% (Cavas-Martinez et al. 2016). This means that while some KC suspects may not be flagged as suspects, nearly everyone who does not have KC will not be flagged as a suspect based on KPI. Screening tests with lower sensitivity are commonly used, and may be interpreted in the context of more information about a patient with clinical decision-making by a provider being relevant to determine whether further testing is still

warranted (Pewsner et al. 2004). In order to provide clearer clinical guidelines, the goal of this study was to identify a metric that held positive predictive value in identifying KC.

When taking into consideration the bootstrapped 95% confidence intervals in Figure 8, all models included in this figure were comparable, meaning that statistically none were "better" than any others at predicting KPI. This could indicate that the results of the linear model are uncertain and that another study replicating this would find no difference between the models and therefore no significant findings. It could also indicate that there is simply high variability in performing this type of testing on pediatric patients. There is a certain amount of variability that is expected when working with a pediatric population, but this level of uncertainty is extremely high and warrants further investigation. Additionally, the highest r-squared value produced in this analysis was 0.374.

KC is classically thought to affect patients around or slightly after the onset of puberty, beginning in the second decade of life and progressing until it stabilizes in the third or fourth decade (Buzzonetti et al. 2020). However, KC does occur in younger patients, and pediatric KC may be associated with faster disease progression (Chatzis and Hafezi 2012), though this is contested (Dana et al. 1992; Woodward et al. 1990). The CLEK study found a mean age at diagnosis of 27.3 ± 9.5 years with a range from 10 to 39 years (Anitha et al. 2021; Zadnik et al. 1998).

Linear modeling was used to mathematically determine which data points best predicted KPI, and the model that best predicted KPI, included all data points other than pachymetry, which was excluded from analysis anyway. Literature finds that pachymetry is not as strong a

predictor of visual function in KC as topographic or wavefront information (Bayraktar Bilen et al. 2016). Taking all data points from a comprehensive exam into consideration may be relevant when discussing formal diagnosis of KC, but is much more complex than indicated in screening, which aims to consider a single measurement or reading in order to raise suspicion and warrant further testing.

Other than the model containing all parameters, the models with highest r-squared values included age, AGC, SD, and SAI in slightly varying combinations. The findings of this study indicate that overall KPI and thus suspicion of KC diagnosis is best predicted by considering severity of all topographic, refractive, and aberrometric findings as well as patient age. However, considering simply patient age along with topographic indices corresponding to corneal asymmetry and deviation of power may perform similarly to considering all demographic, topographic, and aberrometric information at predicting KC suspicion.

According to Topcon, the CA-800 topographer calculates KPI based on AK, AGC, and SI (Topcon 2024). It would then make sense that the best predictors of KPI in this study would be AK, AGC, and SI. However, while AGC was found to be one of the best predictors of KPI, AK and SI were not; rather SD and SAI were identified as among the best predictors. This means that while KPI was calculated from certain indices, in reality it was better correlated with others, which suggests that there may be inconsistencies in which corneal features are best described or predicted by this index. While Topcon has released information stating which indices KPI is calculated from, as of this writing there is no information regarding the specific mathematics performed in this calculation. This only adds to the

confusion regarding topographic KC indices. There are different definitions for indices with the same name corresponding to different topographer manufacturers, and even one term across studies or manufacturers does not match what it is purportedly based on. This highlights the need for standardization of topography indices, particularly multivariate indices, in order to describe overall likelihood or severity of KC.

There are limitations to these findings that must be considered. The bootstrap function estimates the distribution of a dataset by random resampling with replacement of data or a model derived from the data, and can provide probabilities for confidence intervals (Horowitz 2001). As seen in Figure 8, the bootstrapped 95% confidence intervals are so wide that they encompass close to the entirety of each model, which may mean that while the findings of this study are valid for the sample size of 164 eyes, the results are very unlikely to be replicated on a much larger scale. Additionally, due to necessary exclusions in this analysis the sample size was smaller than intended based on the a priori power analysis, leaving these results underpowered to detect the hypothesized effect.

This result may also indicate high uncertainty or lack of repeatability in the data collected. In general, pediatric research may involve additional variability and difficulty in obtaining reliable results. Research across various fields of medicine tends to find mixed results regarding validity and reliability of various objective measurements, with more reliable findings resulting from fields that have clearly defined standards for measurements and procedures. In other words, evidence-based methods produce reliable results (Antsygina et al.

2025; Rowland et al. 2020; Weiner and McGrath 2017), including in the field of eye health (DeCarlo et al. 2020).

Topography and aberrometry measurements are known to be affected by KC due to the limitation that intrinsic algorithms in the machines may not accurately measure high amounts of irregularity as occurs in KC, with inaccurate readings up to 4D occurring (Cavas-Martinez et al. 2016). A study comparing the Topcon CA-800 to the Topcon 3D OCT-2000 in terms of tear meniscus height measurement in contact lens wearers found that tear meniscus height measured with this topographer was reliable, but not as accurate as that measured with OCT and the values could not be interchanged (Valencia-Nieto et al. 2024). Anterior segment swept source (SS) OCT has higher repeatability of pachymetry than Scheimpflug imaging in healthy patients (Schroder et al. 2018), and higher reliability and repeatability than Scheimpflug imaging in patients with corneal grafts (Asam et al. 2019). However, these studies are limited to healthy patients; little is known about reliability and repeatability of these types of measurements among a diseased population, such as patients with KC. Additionally, findings in adult populations may not always generalize to pediatric populations, and reliability of these measurements among a diseased pediatric population is also not known. Altogether this means that there is not sufficient data describing the repeatability of the imaging techniques used in this study with regards to this specific population, so our findings should be considered in this context, and further research is needed to determine reliability of these imaging methods.

4.3 Analysis When Grouping by KC Suspects Based On KPI

KPI is accepted as a predictor of KC with the ability to distinguish eyes with KC from those without in 96% of cases (Maeda et al. 1994). A minimum value for KPI of 23% is commonly used as a cutoff for KC suspicion (Maeda et al. 1994), although some KC studies have attempted to classify KC suspects based on their KPI in conjunction with other values and criteria, with a KPI >30% considered a “major criterion” and 23-30% considered a “minor criterion” (Jafarinasab et al. 2015) without taking into account the status of the fellow eye. The status of the fellow eye was also not considered in this study as a criterion in determining KC suspicion, as patients identified as suspects were referred to a specialist for confirmation of diagnosis.

It was expected that subjects identified as KC suspects would be confirmed to have KC upon repeat testing with tomography, and as such display significantly more characteristics associated with KC than the non-suspects group. Common findings in KC include increased myopia and irregular astigmatism, steepening and thinning of the cornea with more irregular shape, as well as increased magnitudes of aberrations such as spherical aberration, coma, and in general, higher order aberrations (Anitha et al. 2021; Buzzonetti et al. 2020; Gobbe and Guillon 2005; Gomes et al. 2015; Krumeich et al. 1998). Thus, it was expected that these measurements would be reflected in the results of this study, with the KC suspect group exhibiting more extreme measurements.

Subjects flagged as KC suspects based on KPI were found to have increased K cyl, steeper steep K, higher SI, higher SAI, have more negative M/SE, more total aberrations, more astigmatism aberrations, and be older.

4.3.1 Topographic Indices

Subjects flagged as KC suspects in this study based on KPI had higher values for the topographic indices corresponding to corneal steepness and more corneal asymmetry, consistent with the hallmark findings of KC of corneal steepening, increased irregular astigmatism, and increased irregularity of the corneal surface (Buzzonetti et al. 2020; Gomes et al 2015). Because both SI and SAI were higher among KC suspects, this indicates that this study found increased overall asymmetry as well as sector-specific asymmetry in KC suspects, which supports current literature consensus.

There were no significant differences between the KC suspects and non-suspects for several data points that were expected to exhibit differences, including topography indices that describe central and maximum corneal steepness, and rate of change of corneal curvature. However, significant differences did exist for indices describing higher corneal steepness (steep K) and more corneal asymmetry (SI and SAI). Steep K and AK both describe corneal steepness, but in slightly different ways - AK is corneal power at the apex, and steep K is the power of the steeper corneal meridian. These results mean that KC suspects had significantly steeper steep corneal meridians, but not necessarily significantly steeper apical corneal power.

KC suspects also did not have more deviation in corneal power (SD) or rate of change of corneal curvature (AGC). These are both features of KC that were expected to differ between the groups in this study. The fact that certain indices were significantly different and others were not may indicate that in this cohort KC suspects tended to exhibit certain expected features of early KC (corneal surface asymmetry) and not others (apical corneal power and rate of change of corneal steepness).

Many topographic indices have been developed in order to describe the shape and curvature of the cornea to identify abnormal corneas and classify KC severity. However, indices tend to be specific to the topographer for which they were developed and direct comparison between indices of different topographers is not possible (Cavas-Martinez et al. 2016). Various univariate indices exist, in which a single aspect of the cornea is described or quantified, and multivariate analyses combine several univariate indices to produce an overall description of the cornea or the likelihood of KC.

With so many different ways of detecting and describing KC, it is difficult to point to a group of specific indices that should be used to detect early KC that can be easily compared across different detection methods. Indicators commonly used with children include changes in max keratometry (Kmax), refractive astigmatism (cyl), and corrected distance VA (CDVA) (Chatzis and Hafezi 2012; Hashemi et al. 2022; Sylvain et al. 2016). This study supports the finding that increased steepening and corneal cyl are indicators of early KC or KC suspicion.

4.3.2 Refractive Error and Vector Components

It can be difficult to measure refractive error in manifest KC, due to irregular astigmatism and more fluctuations in vision and refraction in patients with KC than healthy corneas (Davis et al. 1998; Krumeich et al. 1998). This study did not find significant presence of oblique astigmatism nor significant differences in oblique astigmatism between KC suspects and non suspects, which is slightly surprising as oblique astigmatism is often associated with KC (Kamiya et al. 2015), though conflicting reports exist regarding oblique corneal astigmatism in KC (Naderan et al. 2016).

As KC advances and causes corneal steepening, it is typically associated with increased myopia (Krumeich et al. 1998). Past studies have attempted to classify typical refractive features of early/subclinical KC, but findings are mixed (Castro-Luna and Perez-Rueda 2020). Differences have been found between normal and early subclinical KC in sphere only (Castro-Luna and Perez-Rueda 2020); or the cylinder and not sphere component (Reddy et al. 2014); or no differences at all (Naderan et al. 2018). Altogether the literature suggests that attempting to predict or classify KC by refractive error is not reliable.

This study unfortunately does not provide a clear answer to the question of the role of refractive error in suspicion of KC. However, it does align with the stance that refractive error is not a reliable predictor of KC development in its early stages.

4.3.3 Aberrations

There are different methods of measuring aberrations. Hartmann-Shack wavefront sensors are commonly used to measure both corneal and total ocular aberrations, and these involve projecting a narrow beam of light into the eye and using an array of lenslets to measure the path length difference between the emitted light beam and a standard wavefront, with this difference representing the eye's natural aberrations (Maeda et al. 2002). Higher order aberrations may also be calculated from topography scans by mathematically converting corneal elevation information into wavefronts using Zernike polynomials over a 6mm area (Colak et al. 2016); this method measures only corneal aberrations.

The aberrations measured by the topographer are calculated only based on corneal shape and do not take into account other ocular aberrations, and as such dilation status did not have an effect on this measurement. Aberrations in this study were obtained from the topography scans, which produce maps and measurements associated with anterior corneal aberrations over a specified pupil size, which was 7mm for all subjects in this study. Changing the pupil size affects the aberration map produced, as a larger pupil diameter produces more aberrations than a smaller pupil (Gobbe and Guillon 2005).

Astigmatism aberrations depict how the subject's wavefront is affected by their topography along axes 90º apart; spherical aberration measures how the wavefront is altered by the cornea near the pupil margin compared to the center of the cornea; coma indicates how the wavefront is altered by opposite hemispheres of the cornea; and Topcon describes the HOA

term as a combination of all other aberrations not included in the other measurements (Topcon 2024), meaning it includes an RMS value of all aberrations 3rd order and above.

While total and astigmatism aberrations were found to be significantly higher in KC suspects in this study, higher order aberrations including total HOAs, spherical aberration, and coma were not different between the two groups. It was expected that KC suspects would exhibit more overall aberrations as well as specifically those normally associated with KC, including higher order (HOAs), spherical (SAs), and coma (Buzzonetti et al. 2020; Masiwa and Moodley 2020; Rabinowitz and Rasheed 1999), but no differences were seen between the groups for these.

It has been suggested that since corneal aberrations are the largest source of total aberrations in patients with KC, their measurement should effectively help identify early KC and aid in its classification (Gobbe and Guillon 2005). In a study to detect and quantify KC, total ocular higher order aberrations measured with a videokeratoscope were found to be significantly higher in KC suspects than normal subjects at low luminance with a 6mm pupil, but not significantly different at medium luminance with a 4.5mm pupil or high luminance with a 3mm pupil (Gobbe and Guillon 2005).

Total higher order aberrations, secondary astigmatism, and coma are typically considered the best identifiers of early or forme fruste KC (Gobbe and Guillon 2005; Jafri et al. 2010; Maeda et al. 2002; Omar 2019). Conflicting evidence exists regarding the ability to detect early or suspected KC based on aberrations, and more advanced methods of aberrometry

such as a combination of videokeratography and wavefront aberrometry may be required to differentiate healthy eyes, suspected KC, and manifest KC eyes (Jafri et al. 2010).

This study found that the only corneal aberrometric differences between healthy and suspected KC eyes were total and astigmatism aberrations, and no differences were found for the aberrations typically associated with early KC. This suggests that corneal aberrations alone may not be sufficient to differentiate healthy from suspect KC eyes, and further research should investigate corneal aberrations' compared to total ocular aberrations' ability to identify healthy, suspected KC, and manifest KC eyes.

4.3.4 Age

As age was a significant predictor of KPI in the linear models, and it was significantly different between KC suspects and non-KC suspects, increased age in pediatric patients was found to be associated with KC suspicion.

KC is classically thought to manifest around the onset of puberty, with reports of average age of onset ranging from 10 to 40 (Anitha et al. 2021; Godefrooij et al. 2017). It is rare for KC to affect patients before puberty (Anitha et al. 2021), though it does affect younger patients (Chatzis and Hafezi 2012; Ertan and Muftuoglu 2008). It is thought that the onset of KC is somewhat correlated with puberty, with a possible role of hormones including the sex hormones estrogen and progesterone, and thyroid hormone T4, or thyroxine (Ayan et al. 2019; Thanos et al. 2016). There is a fairly wide reported range of average age of puberty onset, between 8 and 14 years (Hammad et al. 2026), and the average age of KC suspects

(13.07 ± 1.36 years) was significantly higher than non-suspects (10.42 ± 3.56 years), with both groups roughly aligning with the upper and lower bounds of puberty onset.

4.3.5 Summary of Findings When Analyzing by KPI

This study found significant differences between non-KC and suspect KC eyes in the data points SE/M, K cyl, steep K, SI, SAI, total aberrations, astigmatism aberrations, and age. Altogether this study found KC suspicion was correlated with an older age around the onset of puberty, steeper corneas and more asymmetrical corneal curvature, more negative spherical equivalent refractive error, and increased corneal aberrations than patients with healthy corneas. Generally, these findings were expected; however, it was also hypothesized that increased astigmatism would be associated with suspected KC, and while K cyl was significantly higher in KC suspects, there was no difference in J0 or J45, indicating the vector components of regular astigmatism. Altogether this can be taken to mean that when screening patients for KC, corneal topography should be considered in addition to aberrations and overall refraction.

The results of linear modeling show that corneal steepness and rate of change of steepness, represented by AGC, and deviation of corneal power, represented by SD, were significant predictors of KPI. Additionally, KC suspects had significantly higher steep K, as well as surface asymmetry, as represented by SI and SAI being significantly higher among this group. The indices AGC and SD were found to be significant predictors of KPI, but were not found to be significantly different between KC suspects and non-suspects. The indices M, K cyl, steep K, SI, total aberrations, and astigmatism aberrations were found to be significantly

different between KC suspects and non-suspects, but were not significant predictors of KPI. Age and SAI were the only predictors that were significant in both forms of analysis.

The most significant KC predictors describe steepness, asymmetry of shape and power distribution on the cornea, and aberrations, so these should be considered highly when considering KC suspicion. Literature suggests that the most significant features when predicting development of KC are those representing asymmetry of topography, tomography, and pachymetry (Gomes et al. 2015), which is supported by the findings of this study. Topography is a powerful screening tool that can detect corneal asymmetry to flag suspects, and using this along with retinoscopy and consideration of other patient risk factors including age and ocular allergies/eye rubbing may perform similarly well at detecting KC suspects as considering all risk factors and performing further testing.

In order to describe and predict development of KC, it is imperative that a more universally applicable classification scheme and set of descriptors is developed. It appears somewhat redundant to have many different ways of describing subtle differences in asymmetry of the cornea considering that no specific index has proven to be significantly better than another in detecting KC. Other eye diseases, such as diabetic retinopathy, have standardized severity scales with strict cutoffs for different categories of disease state, and specific measurements. For example, as defined by the Early Treatment of Diabetic Retinopathy Study (ETDRS), clinically significant macular edema, or CSME, has strict guidelines for classification regarding exact size and number of clinical findings such as retinal thickening and hard exudates (ETDRS Research Group 1991). While it is true that diabetic retinopathy (DR) and

KC are very different disease entities, and that classification of CSME and DR continues to evolve, it is evident that there are much more specific guidelines and definitions for other diseases.

4.4 Importance of KC Classification

An important part of researching and describing KC includes describing how the disease evolves from subclinical to manifest, and how it then progresses or stabilizes with or without management. Standardization of indices is needed to make universal recommendations about KC detection. However, once this is achieved, there are still barriers to making recommendations regarding KC detection due to lack of a universal classification system and nomenclature. This is a major step that is needed in order to advance KC research. While this study is not extensive enough to propose a classification system, certain corneal features were found to be significant and should be included in future development of a classification system.

While certain corneal features can be identified as good predictors of KC, as discussed previously, due to the lack of standardization of topographic indices it is impossible to make recommendations that can be generalized to any machine. For example, while SI is an index that was found to be significantly different in KC suspects from non-suspects in this study, this index exists on the Topcon CA-800 but not on other machines such as Topographic Modelling System (TMS-1) (Computed Anatomy Inc, New York, USA). This topographer does produce the I-S index, which is similar, but calculations and numerical cutoffs are different between the indices so they cannot be directly compared. Additionally, multivariate

indices that are overall predictors of KC are then calculated from these different univariate indices, so they are even less comparable than the univariate indices.

Various proposed KC classification systems have been supported with clinical research, but none have been accepted as a universal system of classification. They tend to be organized numerically from mild or subclinical disease to severe or advanced, with more severe findings for any data point qualifying the patient for placement in more severe categories. The Belin ABCD system appears to be the only classification scheme for KC that does not offer a single numerical value or letter grade quantifying disease severity, but rather places a patient in a broader category of disease severity based on sub-scores that are composed of numerical severity ratings. This system, while it does not encompass all the necessary points to adequately describe KC based on current technological capabilities, does seem to offer the most comprehensive description of the state of a cornea at risk of KC or exhibiting KC. It also can be displayed in a "change over time" format similar to a GPA progression used in glaucoma to chart and predict future disease progression based on visual field or OCT findings (Tanna et al. 2012).

Diabetic retinopathy is staged according to extensive definitions and guidelines established by the Early Treatment Diabetic Retinopathy Study Research Group, or ETDRS. This study group outlined clear definitions for CSME, as well as severity stages for non-proliferative and proliferative DR based on standard stereoscopic color fundus photographs (ETDRS Research Group 1991). Based on these findings and detailed staging system, a simpler severity scale was created with fewer categories but based on the same rigorously defined

criteria, the International Clinical Disease Severity Scale for DR (Wilkinson et al. 2003; Wu et al. 2013). This grading system is ubiquitous in eye care today, and the simpler severity scale is much more clinically useful, allowing for interprofessional management as needed to manage the overall disease (Frank 2015).

A 2023 paper by Cheung et al. as part of the Neurotrophic Keratopathy Study Group describes an updated staging system of the severity of neurotrophic keratopathy (NK). Stage 1 involves no keratopathy but altered sensation, and is of mild severity with good prognosis. The rest of the stages 2-6 include increasing levels of severity of corneal involvement, with worse prognosis. This staging system was created in order to better address the progression of the disease, as well as defining earlier stages and allowing clinicians to more easily detect early disease. The pathophysiology of NK is multifactorial, and this staging system incorporates features from various contributing factors in order to better describe the overall clinical picture. The updated staging system allows for more detailed understanding of the cause of NK and pathophysiology in a particular patient, and with more research will allow projection of disease progression or prognosis and can inform which treatment modality may be most effective.

These disease staging systems that tend to be successful for other eye conditions may offer a framework for how to stage KC, while taking into consideration the specific nature of KC and how to tailor a grading scheme specifically to this condition. Successful severity scales tend to include a wide range of manifestations of the disease, rather than only a few common or “hallmark” findings. They also may include distinctions between clinical findings and

symptoms, both of which are important to consider and do not always perfectly correlate. Often they also include quantification of certain findings, such as the number of hemorrhages in DR. They also evolve over time and adapt to developments in technology and imaging, incorporating the emerging ability to identify microscopic changes in tissue that would not be identifiable on direct clinical examination. It is also very helpful to include standard photographs in order to demonstrate how certain findings appear clinically, or how severe a finding should appear to be classified at a certain level.

Keratoconus is a multifactorial disease, with many possible presentations and early corneal manifestations. It also can vary widely in degree and type of symptoms. New technology such as AS-OCT is very helpful at viewing the microarchitecture of the cornea and detecting subclinical changes. The Belin classification system offers a good framework for a KC severity classification system, with several points informing one overall grade of severity. The KSS is also informed by a list of detailed findings and requires decision-making by a trained examiner, with a simple numerical score the final product.

KC is difficult to describe in few simplistic categories due to its complex and multifactorial nature. A full description of a patient's disease state includes numerous data points and descriptors, and a successful scale of severity should include an array of variables as risk factors - clinical findings as well as symptoms; imaging including AS-OCT, topography, and tomography; assessment of longitudinal change; and assessment of interocular asymmetry - with weights for each risk factor based on severity to produce a simple overall description of disease severity and prognosis.

4.5 Limitations and Future Research

Because KC is a relatively uncommon condition, the sample size of this study was fairly small. Additionally, due to difficulty regarding patient retention and follow-ups inherent to conducting research via recruitment at a community health center, as well as the time constraints of this project, it was not possible to analyze subjects' change over time to identify progression of characteristics associated with development of KC or corneal stability. Future research should focus on change in data points such as refractive cyl over time to investigate when a certain amount of change in a specific timeframe should be viewed as suspicious for KC. Additionally, due to these limitations and exclusions, the study sample size was lower than determined by the a priori power analysis, meaning that the analysis was likely underpowered to detect the expected effect.

Another statistical limitation of this study is the possible effect of inter-eye correlation as subjects' eyes were analyzed individually - usually, to avoid this either an eye is selected at random or one eye is selected a priori for analysis from each subject, often the right eye by convention. It was not possible to perform analysis in this manner for this thesis due to sample size constraints. Additionally, in future research subjects' eyes should be compared to one another to assess for asymmetry, as well as asymmetric change over time as part of a longitudinal study design. Normality of data was also not tested, and should be incorporated into future studies.

Pachymetry is an important value to consider when screening for KC as the disease typically causes characteristic inferior thinning especially near the apex of the cone

(Santodomingo-Rubido et al. 2022). Additionally, analysis of specific corneal layers, particularly epithelial thickness has been suggested to be particularly relevant in subclinical KC (Li et al. 2012; Li et al. 2016). Pachymetry measurement should be standardized before inclusion in any future studies, as corneal thickness is a vital consideration in KC research. Future pachymetry measurements should include attention to specifically epithelial thickness.

Corneal imaging was also performed after dilation. This can introduce variability in topography scans, as adding a drop to the corneal surface may affect the ability for the topographer to accurately collect data across the subject's cornea. Typically a minimum of about 10 minutes passed between drop instillation and imaging; however this may still affect scan quality, and in the future corneal imaging should be captured before instilling any eye drops.

A follow-up study is planned in partnership with a site that has access to tomography, in order to streamline the process of confirming suspected KC cases, as well as recruit more subjects to strengthen sample size and study power. Confirming cases of KC, incorporating standardized pachymetry measurements, and following subjects over time will provide steps for more robust data collection regarding findings in early KC and how they develop over time, providing data to inform KC severity classification and future nomenclature.

There are several opportunities for further research in the field of KC research as a whole. More research is needed regarding repeatability and reliability of topography, aberrometry, and AS-OCT in pediatric patients with KC and other anterior segment eye diseases. This will allow for more rigorous standards in this field of research and will allow researchers to

obtain valid data and advance knowledge regarding pediatric KC. A larger study with longer follow-up time and longitudinal design would be able to address these limitations and add value to findings. When working with pediatric patients, a certain level of variability and unpredictability is expected, which makes it more difficult to obtain valid results. Additionally, KC is fairly rare, and tends to be an unpredictable condition which can vary in presentation. Altogether this adds to the difficulty in performing clinical research into KC.

KPI in this study was calculated by the Topcon topographer from the indices AK, AGC, and SI. The literature sensitivity and specificity are based on KPI calculated from eight different indices, meaning that the optimized sensitivity and specificity may not occur at the 23% value used in this study. Determining this value is outside the scope of this project, but a future study with a larger sample size should utilize ROC analysis to investigate the Topcon KPI that optimizes sensitivity and specificity.

Several researchers have attempted to create a universal classification scheme for KC, but none have thus far been accepted. However, there are features that are regarded as vital to diagnosing and describing the disease. A global consensus panel on KC outlined the following findings as mandatory for KC diagnosis: abnormal posterior corneal ectasia, abnormal corneal thickness, and corneal thinning not associated with an inflammatory disorder (Gomes et al. 2015). However, they were unable to provide specific values because these vary depending on the technology that is used. This panel suggested that full corneal thickness, or pachymetry, map, clinical slit lamp examination, anterior curvature, or topography, map, and anterior tomography map should be used to identify KC and

differentiate it from other ectatic disorders. Additionally, early or subclinical KC should be detected by either Scheimpflug or OCT tomography, and in order to determine a classification scheme, studies are needed that correlate topographic and tomographic changes with clinical findings and symptoms, such as BCVA.

Proposing a classification system is outside the scope of this project due to limitations in sample size, standardization of data collection, and lack of ability to follow up with subjects and follow disease progression. However, significant findings were identified regarding predictors of KC suspicion. In this study, the strongest predictors of KC suspicion were clinical findings including more negative spherical equivalent refractive error (more negative M); topography findings including increased corneal steepness (higher K cyl and steeper steep K) and more asymmetric topography (higher SI, SAI, AGC, and SD); and increased aberrations (more total and astigmatism aberrations). Data was collected from clinical examination, topography, and pachymetry, which allowed for description and analysis of real-world symptoms and disease manifestation as well as description of anterior corneal curvature and thickness changes.

This study agrees with current literature consensus that KC is best detected by considering symmetry of tomographic and topographic steepening as well as distribution of corneal thickness, and combines these imaging findings with refractive as well as aberrometric data. A successful KC classification system and well-defined nomenclature are necessary in order to provide clearer guidelines regarding detection of early KC and guide its management. Due to the complex and multifactorial nature of KC, this classification system would best be

defined and organized by having input from several data points including descriptions of clinical findings and symptoms, as well as relevant imaging including topography, tomography, pachymetry, AS-OCT imaging of corneal microarchitectural changes, and aberrometry. The Belin classification system offers a good framework for this system, with categories each producing their own sub-score to combine into an overall descriptor that can also be mapped out over time to show changes and project future development. It should be supplemented by these other data points to provide a more comprehensive description of the disease. Additionally, in order to describe topography, there are many different indices that quantify various corneal characteristics and overall likelihood of KC - it is virtually impossible to clearly define standards for KC without agreement on these indices, so a set of topography indices should also be defined that can be calculated across devices from different manufacturers. Once definitions for stages or severity of KC are described, as well as a classification system and universal topographic indices, more detailed recommendations may be made to clinicians regarding screening for early or suspected KC.

5. Conclusions

Overall, refractive astigmatism was not found to be a good predictor of suspected KC. The KC suspects displayed steeper corneas, more irregular corneal surfaces, older age, more negative spherical equivalent refractive error, and more corneal aberrations. However, a standardized nomenclature and a disease classification system are necessary to describe and classify KC suspects or early KC. A KC classification system should be structured based on a combination of clinical findings and imaging including topography, AS-OCT, and aberrometry, and should include detailed descriptions and standard photographs of each disease feature to capture the complex nature of the disease while providing an overall measure of severity. Further research and consensus are needed to better understand early signs of KC, how to classify these signs, and best practices for screening for suspects.

References

Alio, J. L., & Shabayek, M. H. (2006). Corneal Higher Order Aberrations: A Method to Grade Keratoconus. *Journal of Refractive Surgery*, *22*(6), 539–545.

Altemir, I., Pueyo, V., Elía, N., Polo, V., Larrosa, J. M., & Oros, D. (2013). Reproducibility of Optical Coherence Tomography Measurements in Children. *American Journal of Ophthalmology*, *155*(1), 171-176.e1. https://doi.org/10.1016/j.ajo.2012.06.012

Ambrósio, R., Klyce, S. D., & Wilson, S. E. (2003). Corneal Topographic and Pachymetric Screening of Keratorefractive Patients. *Journal of Refractive Surgery*, *19*(1), 24–29. https://doi.org/10.3928/1081-597X-20030101-05

AMBRÓSIO, RENATO. (2011). 3-D Scheimpflug Corneal Tomography. *CATARACT & REFRACTIVE SURGERY TODAY*, 42–44.

Amsler, M. (1946). Kératocône classique et kératocône fruste; arguments unitaires. *Ophthalmologica*, *111*(2–3), 96–101. https://doi.org/10.1159/000300309

Anitha, V., Vanathi, M., Raghavan, A., Rajaraman, R., Ravindran, M., & Tandon, R. (2021). Pediatric keratoconus—Current perspectives and clinical challenges. *Indian Journal of Ophthalmology*, *69*(2), 214. https://doi.org/10.4103/ijo.IJO_1263_20

Antsygina, O., Rollo, S., McRae, N., Chaput, J.-P., & Tremblay, M. S. (2025). Reliability and validity of instruments containing reported sleep measures among children from birth to <5 years of age: A systematic review. *Sleep Medicine Reviews*, *79*, 102023. https://doi.org/10.1016/j.smrv.2024.102023

Arora, R., & Lohchab, M. (2019). Pediatric keratoconus misdiagnosed as meridional amblyopia. *Indian Journal of Ophthalmology*, *67*(4), 551. https://doi.org/10.4103/ijo.IJO_1496_18

Asam, J. S., Polzer, M., Tafreshi, A., Hirnschall, N., & Findl, O. (2019). Anterior Segment OCT. In J. F. Bille (Ed.), *High Resolution Imaging in Microscopy and Ophthalmology: New Frontiers in Biomedical Optics* (pp. 285–299). Springer International Publishing. https://doi.org/10.1007/978-3-030-16638-0_13

Asimellis, G. (2019). Geometrical Optics: Lectures in Optics, Volume 2. Bellingham: SPIE Press.

Asimellis G. (2022) Visual Optics. SPIE Press.

Astle, A. T., Webb, B. S., & McGraw, P. V. (2011). Can perceptual learning be used to treat amblyopia beyond the critical period of visual development? *Ophthalmic and Physiological Optics*, *31*(6), 564–573. https://doi.org/10.1111/j.1475-1313.2011.00873.x

Aumann, S., Donner, S., Fischer, J., & Müller, F. (2019). Optical Coherence Tomography (OCT): Principle and Technical Realization. In J. F. Bille (Ed.), *High Resolution Imaging in Microscopy and Ophthalmology: New Frontiers in Biomedical Optics* (pp. 59–85). Springer International Publishing. https://doi.org/10.1007/978-3-030-16638-0_3

Ayan, B., Yuksel, N., Carhan, A., Gumuşkaya Ocal, B., Akcay, E., Cagil, N., & Asik, M. D. (2019). Evaluation estrogen, progesteron and androgen receptor expressions in corneal epithelium in keratoconus. *Contact Lens and Anterior Eye*, *42*(5), 492–496. https://doi.org/10.1016/j.clae.2018.11.015

Barrett, C., & Loughman, J. (2018). Expanding the traditional role of optometry: Current practice patterns and attitudes to enhanced glaucoma services in Ireland. *Journal of Optometry*, *11*(4), 252–261. https://doi.org/10.1016/j.optom.2018.02.004

Belin, M. W., Harthan, J. S., Eiden, S. B., Morgenstern, A. S., Tullo, W., Gelles, J. D., Block, S. S., Greenstein, S., & Hersh, P. S. (2022). Revised Calculation of the Prevalence of Keratoconus Based on Updated Scheimpflug Corneal Tomography Metrics in a Pediatric Population From a Chicago-Based School Age Vision Clinic. *Eye & Contact Lens*, 10.1097/ICL.0000000000001250. https://doi.org/10.1097/ICL.0000000000001250

Belin, M. W., Jang, H. S., & Borgstrom, M. (2022). Keratoconus: Diagnosis and Staging. *Cornea*, *41*(1), 1. https://doi.org/10.1097/ICO.0000000000002781

Belin, M. W., Kundu, G., Shetty, N., Gupta, K., Mullick, R., & Thakur, P. (2020). ABCD: A new classification for keratoconus. *Indian Journal of Ophthalmology*, *68*(12), 2831–2834. https://doi.org/10.4103/ijo.IJO_2078_20

Belin, M. W., Villavicencio, O. F., & Ambrósio, R. R. J. (2014). Tomographic Parameters for the Detection of Keratoconus: Suggestions for Screening and Treatment Parameters. *Eye & Contact Lens*, *40*(6), 326. https://doi.org/10.1097/ICL.0000000000000077

Blanca, M., Arnau, J., García-Castro, F. J., Alarcón, R., & Bono, R. (2023). Non-normal Data in Repeated Measures ANOVA: Impact on Type I Error and Power. *Psicothema*, *35*, 21–29. https://doi.org/10.7334/psicothema2022.292

Borle K, Gaiser H, Tran A, Lyons S. Identification of Keratoconus in the Presence of Meridional Amblyogenic Risk. Optom Vis Sci 2022;99:E-abstract 225071.

Burns, D. M., Johnston, F. M., Frazer, D. G., Patterson, C., & Jackson, A. J. (2004). Keratoconus: An analysis of corneal asymmetry. *British Journal of Ophthalmology*, *88*(10), 1252–1255. https://doi.org/10.1136/bjo.2003.033670

Buzzonetti, L., Bohringer, D., Liskova, P., Lang, S., & Valente, P. (2020). Keratoconus in Children: A Literature Review. *Cornea*, *39*(12), 1592. https://doi.org/10.1097/ICO.0000000000002420

Carvalho, L. A. (2005). Accuracy of Zernike Polynomials in Characterizing Optical Aberrations and the Corneal Surface of the Eye. *Investigative Ophthalmology & Visual Science*, *46*(6), 1915–1926. https://doi.org/10.1167/iovs.04-1222

Castro-Luna, G., & Pérez-Rueda, A. (2020). A predictive model for early diagnosis of keratoconus. *BMC Ophthalmology*, *20*(1), 263. https://doi.org/10.1186/s12886-020-01531-9

Cavas-Martínez, F., De la Cruz Sánchez, E., Nieto Martínez, J., Fernández Cañavate, F. J., & Fernández-Pacheco, D. G. (2016). Corneal topography in keratoconus: State of the art. *Eye and Vision*, *3*(1), 5. https://doi.org/10.1186/s40662-016-0036-8

Chastang, P. J. M. a, Borderie, V. M. M. a, Carvajal-Gonzalez, S., Rostene, W., & Laroche, L. M. a. (2000). Automated keratoconus detection using the EyeSys videokeratoscope. *Journal of Cataract & Refractive Surgery*, *26*(5), 675–683. https://doi.org/10.1016/S0886-3350(00)00303-5

Chatzis, N., & Hafezi, F. (2012). Progression of Keratoconus and Efficacy of Corneal Collagen Cross-linking in Children and Adolescents. *Journal of Refractive Surgery*, *28*(11), 753–758. https://doi.org/10.3928/1081597X-20121011-01

Cheung, A. Y., Holland, E. J., Lee, W. B., Beckman, K. A., Tu, E., Farid, M., Pepose, J., Gupta, P. K., Fram, N., Mah, F., & Mannis, M. J. (2023). Neurotrophic keratopathy: An updated understanding. *The Ocular Surface*, *30*, 129–138. https://doi.org/10.1016/j.jtos.2023.09.001

Chopra, R., Wagner, S. K., & Keane, P. A. (2021). Optical coherence tomography in the 2020s—Outside the eye clinic. *Eye*, *35*(1), 236–243. https://doi.org/10.1038/s41433-020-01263-6

Colak, H. N., Kantarci, F. A., Yildirim, A., Tatar, M. G., Goker, H., Uslu, H., & Gurler, B. (2016). Comparison of corneal topographic measurements and high order aberrations in keratoconus and normal eyes. *Contact Lens and Anterior Eye*, *39*(5), 380–384. https://doi.org/10.1016/j.clae.2016.06.005

Cotter, S. A. (2006). Treatment of Anisometropic Amblyopia in Children with Refractive Correction. *Ophthalmology*, *113*(6), 895–903. https://doi.org/10.1016/j.ophtha.2006.01.068

Cremasco, F., Massa, G., Vidotti, V. G., de Carvalho Lupinacci, Á. P., & Costa, V. P. (2011). Intrasession, Intersession, and Interexaminer Variabilities of Retinal Nerve Fiber Layer Measurements with Spectral-Domain OCT. *European Journal of Ophthalmology*, *21*(3), 264–270. https://doi.org/10.5301/EJO.2010.5469

Dana, M. R., Putz, J. L., Viana, M. A. G., Sugar, J., & McMahon, T. T. (1992). Contact Lens Failure in Keratoconus Management. *Ophthalmology*, *99*(8), 1187–1192. https://doi.org/10.1016/S0161-6420(92)31825-1

Davis, L. J., Schechtman, K. B., Begley, C. G., Shin, J. A., & Zadnik, K. (1998). Repeatability of refraction and corrected visual acuity in keratoconus. *Optometry and Vision Science*, *75*(12), 887–896. https://doi.org/10.1097/00006324-199812000-00011

de Sanctis, U., Aragno, V., Dalmasso, P., Brusasco, L., & Grignolo, F. (2013). Diagnosis of Subclinical Keratoconus Using Posterior Elevation Measured With 2 Different Methods. *Cornea*, *32*(7), 911. https://doi.org/10.1097/ICO.0b013e3182854774

de Sanctis, Ugo, Loiacono, Carlotta, Richiardi, Lorenzo, Turco, Davide, Mutani, Bernardo, & Grignolo, Federico M. (2008). Sensitivity and Specificity of Posterior Corneal Elevation Measured by Pentacam in Discriminating Keratoconus/Subclinical Keratoconus. *Ophthalmology*, *115*(9), 1534–1539. https://doi.org/10.1016/j.ophtha.2008.02.020

DeCarlo, D. K., Gao, L., McGwin, G., Owsley, C., & Kwon, M. (2020). Repeatability and Validity of MNREAD Test in Children With Vision Impairment. *Translational Vision Science & Technology*, *9*(13), 25. https://doi.org/10.1167/tvst.9.13.25

Deshpande, P. G., Bhalchandra, P. C., Nalgirkar, A. R., & Tathe, S. R. (2018). Improvement of visual acuity in residual meridional amblyopia by astigmatic axis video games. *Indian Journal of Ophthalmology*, *66*(8), 1156. https://doi.org/10.4103/ijo.IJO_1096_17

Dudakova, L., & Jirsova, K. (2013). The impairment of lysyl oxidase in keratoconus and in keratoconus-associated disorders. *Journal of Neural Transmission*, *120*(6), 977–982. https://doi.org/10.1007/s00702-013-0993-1

Early Treatment Diabetic Retinopathy Study Research Group. (1991). Grading Diabetic Retinopathy from Stereoscopic Color Fundus Photographs—An Extension of the Modified

Airlie House Classification: ETDRS Report Number 10. *Ophthalmology*, *98*(5, Supplement), 786–806. https://doi.org/10.1016/S0161-6420(13)38012-9

Efron, N., & Hollingsworth, J. G. (2008). New perspectives on keratoconus as revealed by corneal confocal microscopy. *Clinical and Experimental Optometry*, *91*(1), 34–55. https://doi.org/10.1111/j.1444-0938.2007.00195.x

El Rami, H., Chelala, E., Dirani, A., Fadlallah, A., Fakhoury, H., Cherfan, C., Cherfan, G., & Jarade, E. (2015). An Update on the Safety and Efficacy of Corneal Collagen Cross-Linking in Pediatric Keratoconus. *BioMed Research International*, *2015*(1), 257927. https://doi.org/10.1155/2015/257927

El-Agha, M.-S. H., El Sayed, Y. M., Harhara, R. M., & Essam, H. M. (2014). Correlation of Corneal Endothelial Changes With Different Stages of Keratoconus. *Cornea*, *33*(7), 707. https://doi.org/10.1097/ICO.0000000000000134

Enaholo, E. S., Musa, M. J., & Zeppieri, M. (2025). Objective Refraction Technique: Retinoscopy. In *StatPearls*. StatPearls Publishing. http://www.ncbi.nlm.nih.gov/books/NBK597373/

Fozailoff, A., Tarczy-Hornoch, K., Cotter, S., Wen, G., Lin, J., Borchert, M., Azen, S., & Varma, R. (2011). Prevalence of Astigmatism in 6- to 72-Month-Old African American and Hispanic Children: The Multi-Ethnic Pediatric Eye Disease Study. *Ophthalmology*, *118*(2), 284–293. https://doi.org/10.1016/j.ophtha.2010.06.038

Frank, R. N. (2015). Diabetic Retinopathy and Systemic Factors. *Middle East African Journal of Ophthalmology*, *22*(2), 151. https://doi.org/10.4103/0974-9233.154388

Garcia-Ferrer, F. J., Akpek, E. K., Amescua, G., Farid, M., Lin, A., Rhee, M. K., Varu, D. M., Musch, D. C., Mah, F. S., & Dunn, S. P. (2019). Corneal Ectasia Preferred Practice Pattern®. *Ophthalmology*, *126*(1), P170–P215. https://doi.org/10.1016/j.ophtha.2018.10.021

Giannaccare, G., Murano, G., Carnevali, A., Yu, A. C., Vaccaro, S., Scuteri, G., Maltese, L., & Scorcia, V. (2021). Comparison of Amsler–Krumeich and Sandali Classifications for Staging Eyes with Keratoconus. *Applied Sciences*, *11*(9), Article 9. https://doi.org/10.3390/app11094007

Gobbe, M., & Guillon, M. (2005). Corneal wavefront aberration measurements to detect keratoconus patients. *Contact Lens and Anterior Eye*, *28*(2), 57–66. https://doi.org/10.1016/j.clae.2004.12.001

Godefrooij, D. A., de Wit, G. A., Uiterwaal, C. S., Imhof, S. M., & Wisse, R. P. L. (2017). Age-specific Incidence and Prevalence of Keratoconus: A Nationwide Registration Study. *American Journal of Ophthalmology*, *175*, 169–172. https://doi.org/10.1016/j.ajo.2016.12.015

Goggin, M., Alpins, N., & Schmid, L. M. (2000). Management of irregular astigmatism. *Current Opinion in Ophthalmology*, *11*(4), 260.

Goldsmith, J. A., Li, Y., Chalita, M. R., Westphal, V., Patil, C. A., Rollins, A. M., Izatt, J. A., & Huang, D. (2005). Anterior chamber width measurement by high-speed optical coherence tomography. *Ophthalmology*, *112*(2), 238–244. https://doi.org/10.1016/j.ophtha.2004.09.019

Gomes, J. A. P., Rodrigues, P. F., & Lamazales, L. L. (2022). Keratoconus epidemiology: A review. *Saudi Journal of Ophthalmology*, *36*(1), 3. https://doi.org/10.4103/sjopt.sjopt_204_21

Gomes, J. A. P., Tan, D., Rapuano, C. J., Belin, M. W., Ambrósio, R. J., Guell, J. L., Malecaze, F., Nishida, K., Sangwan, V. S., & Diseases, the G. of P. for the G. D. P. of K. and E. (2015). Global Consensus on Keratoconus and Ectatic Diseases. *Cornea*, *34*(4), 359. https://doi.org/10.1097/ICO.0000000000000408

Gupta, A., Stead, T. S., & Ganti, L. (2024). Determining a Meaningful R-squared Value in Clinical Medicine. *Academic Medicine & Surgery*. https://doi.org/10.62186/001c.125154

Gupta, Y., Saxena, R., Jhanji, V., Maharana, P. K., Sinha, R., Agarwal, T., Titiyal, J. S., & Sharma, N. (2022). Management Outcomes in Pediatric Keratoconus: Childhood Keratoconus Study. *Journal of Ophthalmology*, *2022*, e4021288. https://doi.org/10.1155/2022/4021288

Hammad, W. B., Nwachukwu, O. A., Abushama, M., Ahmed, B., & Konje, J. C. (2026). Precocious puberty: An overview of pathogenesis, clinical presentation, and management. *Best Practice & Research Clinical Obstetrics & Gynaecology*, *106*, 102716. https://doi.org/10.1016/j.bpobgyn.2026.102716

Harthan, J. S., Gelles, J. D., Block, S. S., Tullo, W., Morgenstern, A. S., Su, B., Chung, D., Yu, A., Greenstein, S. A., Hersh, P. S., & Eiden, S. B. (2024). Prevalence of Keratoconus Based on Scheimpflug Corneal Tomography Metrics in a Pediatric Population From a Chicago-Based School Age Vision Clinic. *Eye & Contact Lens*, *50*(3), 121. https://doi.org/10.1097/ICL.0000000000001072

Hashem, A. O., Aziz, B. F., Wahba, S. S., Roshdy, M. M., & Elawamry, A. I. (2023). Diagnostic accuracy of different keratoconus detection indices of pentacam in paediatric eyes. *Eye*, *37*(6), 1130–1138. https://doi.org/10.1038/s41433-022-02070-x

Hashemi, H., Heydarian, S., Hooshmand, E., Saatchi, M., Yekta, A., Aghamirsalim, M., Valadkhan, M., Mortazavi, M., Hashemi, A., & Khabazkhoob, M. (2020). The Prevalence and Risk Factors for Keratoconus: A Systematic Review and Meta-Analysis. *Cornea*, *39*(2), 263. https://doi.org/10.1097/ICO.0000000000002150

Hashemi, H., Panahi, P., Asgari, S., Emamian, M. H., Mehravaran, S., & Fotouhi, A. (2022). Best Indicators for Detecting Keratoconus Progression in Children: A Report From the Shahroud Schoolchildren Eye Cohort Study. *Cornea*, *41*(4), 450. https://doi.org/10.1097/ICO.0000000000002896

Hofstetter, Henry W. (1959). A KERATOSCOPIC SURVEY OF 13,395 EYES*: Optometry and Vision Science (Pt. 3-11). *Ovid*, *36*(1). https://www.ovid.com/jnls/optvissci/fulltext/00006324-195901000-00001~a-keratoscopic-survey-of-13395-eyes

Horowitz, Joel. (2001). The Bootstrap. In *Handbook of Econometrics* (Vol. 5, pp. 3159–3228). Elsevier. https://doi.org/10.1016/S1573-4412(01)05005-X

Huseynli, S., & Abdulaliyeva, F. (2018). Evaluation of Scheimpflug Tomography Parameters in Subclinical Keratoconus, Clinical Keratoconus and Normal Caucasian Eyes. *Turkish Journal of Ophthalmology*, *48*(3), 99–108. https://doi.org/10.4274/tjo.89587

Jafari, M., & Ansari-Pour, N. (2019). Why, When and How to Adjust Your P Values? *Cell Journal (Yakhteh)*, *20*(4), 604–607. https://doi.org/10.22074/cellj.2019.5992

Jafarinasab, M. R., Shirzadeh, E., Feizi, S., Karimian, F., Akaberi, A., & Hasanpour, H. (2015). Sensitivity and Specificity of Posterior and Anterior Corneal Elevation Measured by

Orbscan in Diagnosis of Clinical and Subclinical Keratoconus. *Journal of Ophthalmic & Vision Research*, *10*(1), 10–15. https://doi.org/10.4103/2008-322X.156085

Jafri, Batool, Li, Xiaohui, Yang, Huiying, & Rabinowitz, Yaron. (2007). Higher Order Wavefront Aberrations and Topography in Early and Suspected Keratoconus. *Journal of Refractive Surgery*, *23*(10). https://journals.healio.com/doi/10.3928/1081-597X-20071001-06

Jindal, A., Ctori, I., Fidalgo, B., Dabasia, P., Balaskas, K., & Lawrenson, J. G. (2019). Impact of optical coherence tomography on diagnostic decision-making by UK community optometrists: A clinical vignette study. *Ophthalmic and Physiological Optics*, *39*(3), 205–215. https://doi.org/10.1111/opo.12613

Kamiya, K., Shimizu, K., Igarashi, A., & Miyake, T. (2015). Assessment of Anterior, Posterior, and Total Central Corneal Astigmatism in Eyes With Keratoconus. *American Journal of Ophthalmology*, *160*(5), 851-857.e1. https://doi.org/10.1016/j.ajo.2015.08.016

Kennedy, R. H., Bourne, W. M., & Dyer, J. A. (1986). A 48-Year Clinical and Epidemiologic Study of Keratoconus. *American Journal of Ophthalmology*, *101*(3), 267–273. https://doi.org/10.1016/0002-9394(86)90817-2

Klyce, S. D. (2009). Chasing the suspect: Keratoconus. *British Journal of Ophthalmology*, *93*(7), 845–847. https://doi.org/10.1136/bjo.2008.147371

Krachmer, J. H., Feder, R. S., & Belin, M. W. (1984). Keratoconus and related noninflammatory corneal thinning disorders. *Survey of Ophthalmology*, *28*(4), 293–322. https://doi.org/10.1016/0039-6257(84)90094-8

Krumeich, J. H., Daniel, J., & Knülle, A. (1998). Live-epikeratophakia for keratoconus. *Journal of Cataract & Refractive Surgery*, *24*(4), 456. https://doi.org/10.1016/S0886-3350(98)80284-8

Kymes, S. M., Walline, J. J., Zadnik, K., & Gordon, M. O. (2004). Quality of life in keratoconus. *American Journal of Ophthalmology*, *138*(4), 527–535. https://doi.org/10.1016/j.ajo.2004.04.031

Lavinsky, F., & Lavinsky, D. (2016). Novel perspectives on swept-source optical coherence tomography. *International Journal of Retina and Vitreous*, *2*(1), 25. https://doi.org/10.1186/s40942-016-0050-y

Léoni-Mesplié, S., Mortemousque, B., Touboul, D., Malet, F., Praud, D., Mesplié, N., & Colin, J. (2012). Scalability and Severity of Keratoconus in Children. *American Journal of Ophthalmology*, *154*(1), 56-62.e1. https://doi.org/10.1016/j.ajo.2012.01.025

Levi, D. M. (2005). Perceptual learning in adults with amblyopia: A reevaluation of critical periods in human vision. *Developmental Psychobiology*, *46*(3), 222–232. https://doi.org/10.1002/dev.20050

Li, X., Yang, H., & Rabinowitz, Y. S. (2009). Keratoconus: Classification scheme based on videokeratography and clinical signs. *Journal of Cataract & Refractive Surgery*, *35*(9), 1597. https://doi.org/10.1016/j.jcrs.2009.03.050

Li, Y., Chamberlain, W., Tan, O., Brass, R., Weiss, J. L., & Huang, D. (2016). Subclinical keratoconus detection by pattern analysis of corneal and epithelial thickness maps with optical coherence tomography. *Journal of Cataract & Refractive Surgery*, *42*(2), 284–295. https://doi.org/10.1016/j.jcrs.2015.09.021

Li, Y., Shekhar, R., & Huang, D. (2006). Corneal Pachymetry Mapping with High-speed Optical Coherence Tomography. *Ophthalmology*, *113*(5), 792-799.e2. https://doi.org/10.1016/j.ophtha.2006.01.048

Li, Y., Tan, O., Brass, R., Weiss, J. L., & Huang, D. (2012). Corneal Epithelial Thickness Mapping by Fourier-Domain Optical Coherence Tomography in Normal and Keratoconic Eyes. *Ophthalmology*, *119*(12), 2425–2433. https://doi.org/10.1016/j.ophtha.2012.06.023

Liu, Y.-C., Chou, P., Wojciechowski, R., Lin, P.-Y., Liu, C. J.-L., Chen, S.-J., Liu, J.-H., Hsu, W.-M., & Cheng, C.-Y. (2011). Power Vector Analysis of Refractive, Corneal, and Internal Astigmatism in an Elderly Chinese Population: The Shihpai Eye Study. *Investigative Ophthalmology & Visual Science*, *52*(13), 9651–9657. https://doi.org/10.1167/iovs.11-7641

Maeda, N., Fujikado, T., Kuroda, T., Mihashi, T., Hirohara, Y., Nishida, K., Watanabe, H., & Tano, Y. (2002). Wavefront aberrations measured with Hartmann-Shack sensor in patients with keratoconus. *Ophthalmology*, *109*(11), 1996–2003. https://doi.org/10.1016/S0161-6420(02)01279-4

Maeda, N., Klyce, S. D., Smolek, M. K., & Thompson, H. W. (1994). Automated keratoconus screening with corneal topography analysis. *Investigative Ophthalmology & Visual Science*, *35*(6), 2749–2757.

Masiwa, L. E., & Moodley, V. (2020). A review of corneal imaging methods for the early diagnosis of pre-clinical Keratoconus. *Journal of Optometry*, *13*(4), 269–275. https://doi.org/10.1016/j.optom.2019.11.001

McMahon, T. T. O., Szczotka-Flynn, L. O., Barr, J. T. O., Anderson, R. J., Slaughter, M. E., Lass, J. H., Iyengar, S. K., & Group, and the C. S. (2006). A New Method for Grading the

Severity of Keratoconus: The Keratoconus Severity Score (KSS). *Cornea*, *25*(7), 794–800. https://doi.org/10.1097/01.ico.0000226359.26678.d1

Mocan, M. C., Yilmaz, P. T., Irkec, M., & Orhan, M. (2008). In vivo Confocal Microscopy for the Evaluation of Corneal Microstructure in Keratoconus. *Current Eye Research*, *33*(11–12), 933–939. https://doi.org/10.1080/02713680802439219

Mukhtar, S., & Ambati, B. K. (2018). Pediatric keratoconus: A review of the literature. *International Ophthalmology*, *38*(5), 2257–2266. https://doi.org/10.1007/s10792-017-0699-8

Multi-Ethnic Pediatric Eye Disease Study (MEPEDS) Group. (2009). Prevalence and Causes of Visual Impairment in African-American and Hispanic Preschool Children: The Multi-Ethnic Pediatric Eye Disease Study. *Ophthalmology*, *116*(10), 1990-2000.e1. https://doi.org/10.1016/j.ophtha.2009.03.027

Myint, J., Edgar, D. F., Kotecha, A., Murdoch, I. E., & Lawrenson, J. G. (2011). A national survey of diagnostic tests reported by UK community optometrists for the detection of chronic open angle glaucoma. *Ophthalmic and Physiological Optics*, *31*(4), 353–359. https://doi.org/10.1111/j.1475-1313.2011.00844.x

Naderan, M., Jahanrad, A., & Farjadnia, M. (2018). Ocular, corneal, and internal aberrations in eyes with keratoconus, forme fruste keratoconus, and healthy eyes. *International Ophthalmology*, *38*(4), 1565–1573. https://doi.org/10.1007/s10792-017-0620-5

Naderan, M., Rajabi, M. T., & Zarrinbakhsh, P. (2016). Distribution of Anterior and Posterior Corneal Astigmatism in Eyes With Keratoconus. *American Journal of Ophthalmology*, *167*, 79–87. https://doi.org/10.1016/j.ajo.2016.03.051

Nughays, R. O., Bazayd, A. S., Alshamekh, L. A., Alshammari, R. A., Alanazi, M. A., Dahlan, H. Y., Alsubhi, J. A., Alshammri, S. G., AlQurashi, N. A., Aldajani, A. H., Alrammah, A. H., Alenezi, M. N., Almutairi, A. A., Alomayri, A. F., & Alghamdi, S. (2025). Efficacy and Safety of Epi-On vs Epi-Off Corneal Cross-Linking in Corneal Ectasia: A Systematic Review and Meta-Analysis of Randomized Controlled Trials. *Clinical Ophthalmology*, *19*, 1531–1541. https://doi.org/10.2147/OPTH.S508618

Omar, I. A. N. (2019). Keratoconus Screening Among Myopic Children. *Clinical Ophthalmology*, *13*, 1909–1912. https://doi.org/10.2147/OPTH.S225326

Ommani, A., Hutchings, N., Thapa, D., & Lakshminarayanan, V. (2014). Pupil scaling for the estimation of aberrations in natural pupils. *Optometry and Vision Science: Official Publication of the American Academy of Optometry*, *91*(10), 1175–1182. https://doi.org/10.1097/OPX.0000000000000369

Patel, R. P., Petrushkin, H., Etherton, K., Terence, K., Dick, A. D., Rahi, J. S., & Solebo, A. L. (2024). Quality assessment of anterior segment OCT images: Development and validation of quality criteria. *Photodiagnosis and Photodynamic Therapy*, *45*, 103886. https://doi.org/10.1016/j.pdpdt.2023.103886

Pesudovs, K., Parker, K. E., Cheng, H., & Applegate, R. A. (2007). The Precision of Wavefront Refraction Compared to Subjective Refraction and Autorefraction. *Optometry and Vision Science*, *84*(5), 387. https://doi.org/10.1097/OPX.0b013e31804f81a9

Pewsner, D., Battaglia, M., Minder, C., Marx, A., Bucher, H. C., & Egger, M. (2004). Ruling a diagnosis in or out with “SpPIn” and “SnNOut”: A note of caution. *BMJ*, *329*(7459), 209–213. https://doi.org/10.1136/bmj.329.7459.209

Rabinowitz, Y. S. M. a, & Rasheed, K. M. (1999). KISA% index: A quantitative videokeratography algorithm embodying minimal topographic criteria for diagnosing keratoconus. *Journal of Cataract & Refractive Surgery*, *25*(10), 1327–1335. https://doi.org/10.1016/S0886-3350(99)00195-9

Rabinowitz, Y. S. (1995). Videokeratographic Indices to Aid in Screening for Keratoconus. *Journal of Refractive Surgery*, *11*(5), 371–406. https://doi.org/10.3928/1081-597X-19950901-14

Radhakrishnan, S., Rollins, A. M., Roth, J. E., Yazdanfar, S., Westphal, V., Bardenstein, D. S., & Izatt, J. A. (2001). Real-Time Optical Coherence Tomography of the Anterior Segment at 1310 nm. *Archives of Ophthalmology*, *119*(8), 1179–1185. https://doi.org/10.1001/archopht.119.8.1179

Ramesh, P. V., Jha, K. N., & Srikanth, K. (2017). Comparison of Central Corneal Thickness using Anterior Segment Optical Coherence Tomography Versus Ultrasound Pachymetry. *Journal of Clinical and Diagnostic Research : JCDR*, *11*(8), NC08-NC11. https://doi.org/10.7860/JCDR/2017/25595.10420

Read, S. A., Collins, M. J., & Carney, L. G. (2007). A review of astigmatism and its possible genesis. *Clinical and Experimental Optometry*, *90*(1), 5–19. https://doi.org/10.1111/j.1444-0938.2007.00112.x

Reddy, J. C., Rapuano, C. J., Cater, J. R., Suri, K., Nagra, P. K., & Hammersmith, K. M. (2014). Comparative evaluation of dual Scheimpflug imaging parameters in keratoconus, early keratoconus, and normal eyes. *Journal of Cataract & Refractive Surgery*, *40*(4), 582. https://doi.org/10.1016/j.jcrs.2013.08.061

Romero-Jiménez, M., Santodomingo-Rubido, J., & Wolffsohn, J. S. (2010). Keratoconus: A review. *Contact Lens and Anterior Eye*, *33*(4), 157–166. https://doi.org/10.1016/j.clae.2010.04.006

Rowland, M., McGee, A., Broderick, A., Drumm, B., Connolly, L., Daly, L. E., Drummond, J., Fitzpatrick, E., Linnane, B., McCormick, P. A., McNally, P., Rainford, L., & Bourke, B. (2020). Repeatability of transient elastography in children. *Pediatric Research*, *88*(4), 587–592. https://doi.org/10.1038/s41390-020-0916-4

Salomão, M., Hoffling-Lima, A. L., Lopes, B., Belin, M. W., Sena, N., Dawson, D. G., & Ambrósio, R. (2018). Recent developments in keratoconus diagnosis. *Expert Review of Ophthalmology*, *13*(6), 329–341. https://doi.org/10.1080/17469899.2018.1555036

Sandali, O., El Sanharawi, M., Temstet, C., Hamiche, T., Galan, A., Ghouali, W., Goemaere, I., Basli, E., Borderie, V., & Laroche, L. (2013). Fourier-Domain Optical Coherence Tomography Imaging in Keratoconus: A Corneal Structural Classification. *Ophthalmology*, *120*(12), 2403–2412. https://doi.org/10.1016/j.ophtha.2013.05.027

Santodomingo-Rubido, J., Carracedo, G., Suzaki, A., Villa-Collar, C., Vincent, S. J., & Wolffsohn, J. S. (2022). Keratoconus: An updated review. *Contact Lens and Anterior Eye*, *45*(3), 101559. https://doi.org/10.1016/j.clae.2021.101559

Scheiman, M., Hertle, R., Beck, R., Edwards, A., Birch, E., Cotter, S., Crouch ER Jr, Cruz, O., Davitt, B., Donahue, S., Holmes, J., Lyon, D., Repka, M., Sala, N., Silbert, D., Suh, D., Tamkins, S., & Pediatric Eye Disease Investigator Group. (2005). Randomized trial of treatment of amblyopia in children aged 7 to 17 years. *Archives of Ophthalmology (Chicago, Ill. : 1960)*, *123*(4), 437–447. https://doi.org/10.1001/archopht.123.4.437

Schröder, S., Mäurer, S., Eppig, T., Seitz, B., Rubly, K., & Langenbucher, A. (2018). Comparison of Corneal Tomography: Repeatability, Precision, Misalignment, Mean Elevation, and Mean Pachymetry. *Current Eye Research*, *43*(6), 709–716. https://doi.org/10.1080/02713683.2018.1441873

Shan, J., DeBoer, C., & Xu, B. Y. (2019). Anterior Segment Optical Coherence Tomography: Applications for Clinical Care and Scientific Research. *Asia-Pacific Journal of Ophthalmology (Philadelphia, Pa.)*, *8*(2), 146–157. https://doi.org/10.22608/APO.201910

Shankar, H., Taranath, D., Santhirathelagan, C. T., & Pesudovs, K. (2008). Repeatability of corneal first-surface wavefront aberrations measured with Pentacam corneal topography. *Journal of Cataract & Refractive Surgery*, *34*(5), 727–734. https://doi.org/10.1016/j.jcrs.2007.11.056

Shi, Y. (2016). Strategies for improving the early diagnosis of keratoconus. *Clinical Optometry*, *8*, 13–21. https://doi.org/10.2147/OPTO.S63486

Smolek, M. K., & Klyce, S. D. (1997). Current keratoconus detection methods compared with a neural network approach. *Investigative Ophthalmology & Visual Science*, *38*(11), 2290–2299.

Stein, J. D., Talwar, N., LaVerne, A. M., Nan, B., & Lichter, P. R. (2012). Trends in Use of Ancillary Glaucoma Tests for Patients with Open-Angle Glaucoma from 2001 to 2009. *Ophthalmology*, *119*(4), 748–758. https://doi.org/10.1016/j.ophtha.2011.09.045

Steinberg, J., Aubke-Schultz, S., Frings, A., Hülle, J., Druchkiv, V., Richard, G., Katz, T., & Linke, S. J. (2015). Correlation of the KISA% index and Scheimpflug tomography in

‘normal’, ‘subclinical’, ‘keratoconus-suspect’ and ‘clinically manifest’ keratoconus eyes. *Acta Ophthalmologica*, *93*(3), e199–e207. https://doi.org/10.1111/aos.12590

Sylvain el-Khoury, MD, Youssef Abdelmassih, MD, Adib Hamade, MD, Elise Slim, MD, Carole G. Cherfan, MD, Elias Chelala, MD, Jamal Bleik, MD, and Elias F. Jarade, MD. (2016, May 13). *Pediatric Keratoconus in a Tertiary Referral Center: Incidence, Presentation, Risk Factors, and Treatment*. Journal of Refractive Surgery. https://journals.healio.com/doi/10.3928/1081597X-20160513-01

Tanna, A. P., Budenz, D. L., Bandi, J., Feuer, W. J., Feldman, R. M., Herndon, L. W., Rhee, D. J., Whiteside-de Vos, J., Huang, J., & Anderson, D. R. (2012). Glaucoma Progression Analysis Software Compared with Expert Consensus Opinion in the Detection of Visual Field Progression in Glaucoma. *Ophthalmology*, *119*(3), 468–473. https://doi.org/10.1016/j.ophtha.2011.08.041

Thanos, S., Oellers, P., Meyer zu Hörste, M., Prokosch, V., Schlatt, S., Seitz, B., & Gatzioufas, Z. (2016). Role of Thyroxine in the Development of Keratoconus. *Cornea*, *35*(10), 1338. https://doi.org/10.1097/ICO.0000000000000988

The Pediatric Eye Disease Investigator Group. (2002). The Clinical Profile of Moderate Amblyopia in Children Younger Than 7 Years. *Archives of Ophthalmology*, *120*(3), 281–287. https://doi.org/10.1001/archopht.120.3.281

Topcon Healthcare. (2024). Topcon CA-800: Reviewing Anterior Corneal Aberrations [Video]. YouTube. https://www.youtube.com/watch?v=EommIe1FjbA.

Topcon Healthcare. (2024). Topcon CA-800: Reviewing Corneal Topography Maps [Video]. YouTube. https://www.youtube.com/watch?v=oIvQnV-_vJM.

Toprak, I., Cavas, F., Velázquez, J. S., Alió del Barrio, J. L., & Alió, J. L. (2021). Three-Dimensional Morphogeometric and Volumetric Characterization of Cornea in Pediatric Patients With Early Keratoconus. *American Journal of Ophthalmology*, *222*, 102–111. https://doi.org/10.1016/j.ajo.2020.09.031

Uçakhan, Ö. Ö., Çetinkor, V., Özkan, M., & Kanpolat, A. (2011). Evaluation of Scheimpflug imaging parameters in subclinical keratoconus, keratoconus, and normal eyes. *Journal of Cataract & Refractive Surgery*, *37*(6), 1116–1124. https://doi.org/10.1016/j.jcrs.2010.12.049

Uçakhan, Ö. Ö., Kanpolat, A., Ylmaz, N., & Özkan, M. (2006). In Vivo Confocal Microscopy Findings in Keratoconus. *Eye & Contact Lens*, *32*(4), 183. https://doi.org/10.1097/01.icl.0000189038.74139.4a

Valencia-Nieto, L., López-de la Rosa, A., López-Miguel, A., & González-García, M. J. (2024). Reliability of Tear Meniscus Height Measurements in Contact Lens Wearers and Its Relationship With Discomfort Symptoms. *Eye & Contact Lens*, *50*(9), 410. https://doi.org/10.1097/ICL.0000000000001115

Wajnsztajn, D., Shmueli, O., Zur, K., Frucht-Pery, J., & Solomon, A. (2022). Predicting factors for the efficacy of cross-linking for keratoconus. *PLOS ONE*, *17*(2), e0263528. https://doi.org/10.1371/journal.pone.0263528

Waring, G. O. (1993). Nomenclature for Keratoconus Suspects. *Journal of Refractive Surgery*, *9*(3), 219–222. https://doi.org/10.3928/1081-597X-19930501-13

Weed, K. H., MacEwen, C. J., Cox, A., & McGhee, C. N. J. (2007). Quantitative analysis of corneal microstructure in keratoconus utilising in vivo confocal microscopy. *Eye*, *21*(5), 614–623. https://doi.org/10.1038/sj.eye.6702286

Weiner, O. M., & McGrath, J. J. (2017). Test-Retest Reliability of Pediatric Heart Rate Variability: A Meta-Analysis. *Journal of Psychophysiology*, *31*(1), 6–28. https://doi.org/10.1027/0269-8803/a000161

Wen, G., Tarczy-Hornoch, K., McKean-Cowdin, R., Cotter, S. A., Borchert, M., Lin, J., Kim, J., & Varma, R. (2013). Prevalence of Myopia, Hyperopia, and Astigmatism in Non-Hispanic White and Asian Children: Multi-Ethnic Pediatric Eye Disease Study. *Ophthalmology*, *120*(10), 2109–2116. https://doi.org/10.1016/j.ophtha.2013.06.039

Wilkinson, C. P., Ferris, F. L., Klein, R. E., Lee, P. P., Agardh, C. D., Davis, M., Dills, D., Kampik, A., Pararajasegaram, R., & Verdaguer, J. T. (2003). Proposed international clinical diabetic retinopathy and diabetic macular edema disease severity scales. *Ophthalmology*, *110*(9), 1677–1682. https://doi.org/10.1016/S0161-6420(03)00475-5

Woodward, E. G., Moodaley, L. C., & O'Hagan, A. (1990). Predictors for likelihood of corneal transplantation in keratoconus. *Eye*, *4*(3), 493–496. https://doi.org/10.1038/eye.1990.64

Wu, L., Fernandez-Loaiza, P., Sauma, J., Hernandez-Bogantes, E., & Masis, M. (2013). Classification of diabetic retinopathy and diabetic macular edema. *World Journal of Diabetes*, *4*(6), 290–294. https://doi.org/10.4239/wjd.v4.i6.290

Yip, H., & Chan, E. (2019). Optical coherence tomography imaging in keratoconus. *Clinical and Experimental Optometry*, *102*(3), 218–223. https://doi.org/10.1111/cxo.12874

Yuan, F., Li, H., Yang, J., Li, W., Zhao, K., Luo, L., Fang, X., Wang, J., Chi, W., & Zeng, K. (2025). Associations between ocular parameters and corneal astigmatism in young Chinese

adults: A cross-sectional study. *BMC Ophthalmology*, *25*(1), 512. https://doi.org/10.1186/s12886-025-04339-7

Zadnik, K., Barr, J. T., Edrington, T. B., Everett, D. F., Jameson, M., McMahon, T. T., Shin, J. A., Sterling, J. L., Wagner, H., & Gordon, M. O. (1998). Baseline findings in the Collaborative Longitudinal Evaluation of Keratoconus (CLEK) Study. *Investigative Ophthalmology & Visual Science*, *39*(13), 2537–2546.

Zhao, S. H., Berkowitz, C., Ralay Ranaivo, H., Laurenti, K., Bohnsack, B. L., Basti, S., & Rossen, J. L. (2024). Evaluation of parameters for early detection of pediatric keratoconus. *BMC Ophthalmology*, *24*(1), 463. https://doi.org/10.1186/s12886-024-03714-0

Appendices

Appendix I

Table 1: Summary of Cohort General Findings

Variable	Mean	SD
Refractive Cyl (D)	-2.28	0.94
Age (years)	10.83	3.89
Spherical equivalent refractive error (D)	-0.71	2.43
Kpi	3.24	11.85
K cyl (D)	-2.48	0.87
Steep K (D)	43.90	1.56
AK (D)	44.48	1.89
AGC (D/mm)	1.16	0.58
SD (D)	0.58	0.16
Kc (D)	42.81	1.62
SI (D)	-0.43	0.62
SAI (D)	0.41	0.32
Total Aberrations (μm)	3.12	1.51
Astigmatism Aberrations (μm)	2.57	1.13
Spherical Aberration (μm)	0.49	0.40
Coma (μm)	0.82	0.75
HOA (μm)	1.11	1.29
M (D)	-0.93	1.22
J0 (D)	1.08	0.54
J45 (D)	-0.01	0.26

Appendix II

Table 2: Statistically Significant Differences between Groups divided by Refractive Cyl

	Cyl ≥3.50D		Cyl <3.50D		p-value	95% CIs	
	Mean	SD	Mean	SD		Lower	Upper
N = eyes	43		121				
Refractive cyl * (D)	**-4.42**	**0.89**	**-2.12**	**0.66**	**<0.01**	**-2.60**	**-2.00**
Age (years)	11.09	3.09	10.50	3.78	0.315	-0.57	1.75
Spherical equivalent refractive error (D)	-1.09	1.87	-0.53	2.74	0.137	-1.32	0.18
KPI	7.63	16.78	3.88	12.95	0.188	-1.88	9.39
K cyl * (D)	**-3.94**	**0.90**	**-2.37**	**0.64**	**<0.01**	**-1.87**	**-1.27**
Steep K * (D)	**45.06**	**1.70**	**44.11**	**1.94**	**<0.01**	**0.33**	**1.58**
AK (D)	45.60	1.99	45.30	4.15	0.530	-0.66	1.27
AGC (D/mm)	1.47	0.97	1.59	3.84	0.764	-0.87	0.64
SD (D)	0.68	0.16	0.65	0.57	0.619	-0.09	0.14
Kc (D)	43.17	1.54	43.11	1.90	0.839	-0.52	0.64
SI (D)	-0.48	0.84	-0.46	0.80	0.883	-0.32	0.27
SAI * (D)	**0.62**	**0.56**	**0.42**	**0.33**	**<0.05**	**0.02**	**0.38**
Total aberrations * (µm)	**4.45**	**0.98**	**2.92**	**1.39**	**<0.01**	**0.87**	**2.19**
Astigmatism aberrations * (µm)	**3.79**	**0.84**	**2.37**	**1.07**	**<0.01**	**0.88**	**1.97**
Spherical aberration (µm)	0.49	0.42	0.48	0.37	0.904	-0.24	0.27
Coma (µm)	0.87	0.76	0.76	0.70	0.648	-0.36	0.57
Higher order aberrations (µm)	1.50	1.55	1.06	1.23	0.333	-0.49	1.38
M * (D)	**-1.65**	**0.97**	**-0.79**	**1.37**	**<0.01**	**-1.24**	**-0.47**
J0 * (D)	**2.15**	**0.45**	**1.00**	**0.37**	**<0.01**	**1.00**	**1.31**
J45 (D)	-0.15	0.48	-0.04	0.32	0.163	-0.27	0.05

Bold values with asterisk * indicate significant difference between groups, $p < 0.05$

Appendix III

Table 3: Summary of Significant Linear Models as determined by $p < 0.05$ and adjusted R-squared >0.15

Model	Adj. R squared	p-value	Lower CI	Higher CI
Kpi ~ SD	0.233	6.49E-05	0.038	0.606
Kpi ~ SD+SAI	0.226	2.85E-04	-0.009	0.510
Kpi ~ Age+SAI	0.151	3.84E-03	0.017	0.433
Kpi ~ AGC+SAI	0.151	3.80E-03	-0.001	0.435
Kpi ~ AGC+SD	0.265	6.75E-05	0.076	0.536
Kpi ~ Age+SD	0.311	1.10E-05	0.087	0.631
Kpi ~ Age+AGC	0.294	2.15E-05	0.089	0.579
Kpi ~ AGC+SD+SAI	0.257	2.24E-04	0.047	0.450
Kpi ~ Age+AGC+SAI	0.305	3.81E-05	0.061	0.524
Kpi ~ Age+SD+SAI	0.308	3.44E-05	0.027	0.557
Kpi ~ Age+AGC+SD	0.374	2.31E-06	0.110	0.627
Kpi ~ Age+AGC+SD+SAI	0.369	7.11E-06	0.109	0.547
Kpi ~ List	0.418	5.95E-04	0.076	0.562

Note: “List” contains model parameters Age, Steep K, AK, AGC, SD, Kc, SI, SAI, K cyl, M, J0, J45, Total Aberrations, Astigmatism Aberrations, SA, Coma, HOA

Appendix IV

Table 4: Statistically Significant Differences between Groups divided by KPI

	KPI ≥23%		KPI <23%		p-value	95% CIs	
	Mean	SD	Mean	SD		Lower	Upper
N = eyes	15		149				
Refractive cyl (D)	-3.07	1.36	-2.69	1.24	0.316	-1.15	0.40
Age * (years)	**13.07**	**3.41**	**10.42**	**3.55**	**<0.05**	**-0.57**	**1.75**
Spherical equivalent refractive error * (D)	**-1.38**	**1.00**	**-0.60**	**2.64**	**<0.05**	**-1.46**	**-0.10**
KPI *	**45.47**	**16.51**	**0.75**	**2.82**	**<0.01**	**35.57**	**53.87**
K cyl * (D)	**-3.58**	**1.32**	**-2.70**	**0.93**	**<0.05**	**-1.62**	**-0.14**
Steep K * (D)	**45.45**	**2.03**	**44.25**	**1.88**	**<0.05**	**0.04**	**2.36**
AK (D)	49.51	9.36	44.98	2.33	0.094	-0.89	9.94
AGC (D/mm)	5.38	10.75	1.19	0.61	0.169	-2.03	10.39
SD (D)	1.19	1.50	0.61	0.16	0.155	-0.25	1.41
Kc (D)	43.62	1.87	43.07	1.80	0.295	-0.52	1.62
SI * (D)	**-1.13**	**1.27**	**-0.40**	**0.72**	**<0.05**	**-1.44**	**-0.02**
SAI * (D)	**0.91**	**0.87**	**0.42**	**0.30**	**<0.05**	**0.01**	**0.97**
Total aberrations * (µm)	**4.29**	**1.35**	**3.09**	**1.41**	**<0.05**	**0.05**	**2.35**
Astigmatism aberrations * (µm)	**3.82**	**1.47**	**2.50**	**1.05**	**<0.05**	**0.08**	**2.56**
Spherical aberration (µm)	0.62	0.59	0.46	0.35	0.500	-0.35	0.65
Coma (µm)	0.67	0.69	0.80	0.72	0.620	-0.72	0.45
Higher order aberrations (µm)	1.28	0.99	1.13	1.34	0.716	-0.71	1.00
M * (D)	**-1.46**	**0.65**	**-0.97**	**1.38**	**<0.05**	**-0.90**	**-0.07**
J0 (D)	1.49	0.70	1.28	0.64	0.271	-0.18	0.61
J45 (D)	-0.05	0.33	-0.07	0.37	0.837	-0.17	0.21

Bold values with one asterisk * indicate significant difference between groups $p < 0.05$